

UNITED STATES DEPARTMENT OF THE INTERIOR

GEOLOGICAL SURVEY

GEOTECHNICAL PROPERTIES OF SAMPLES

FROM BORINGS OBTAINED IN THE

CHUKCHI SEA, ALASKA

by

William J. Winters

and

Homa J. Lee

Open-File Report

85-23

Menlo Park, California 94025

December 1984

This report is preliminary and has not been reviewed for conformity with U.S. Geological Survey editorial standards and stratigraphic nomenclature. Any use of trade names is for descriptive purposes only and does not imply endorsement by the USGS.

## INTRODUCTION:

This report summarizes the geotechnical properties of samples from seven borings that were obtained by the U.S. Geological Survey in the Chukchi Sea during September 1983. Geotechnical tests were performed both at sea and in a shore-based laboratory to measure down-hole variations in physical and geotechnical properties. Stratigraphic interpretation of the nearly continuous sediment and rock samples is presently underway.

Hope basin underlies much of the southern Chukchi Sea. The northern part of Hope basin is bounded by Herald arch, an uplifted welt of Paleozoic and Mesozoic bedrock (Grantz and others, 1975, Holmes and Creager, 1981). Another sedimentary basin, the North Chukchi basin, lies north of Herald arch. Two closely spaced borings were located in the northern margin of Hope basin, two holes (spaced 7 meters apart) were in the southern North Chukchi basin, and the remaining three holes were on Herald arch (Table 1).

## SHIPBOARD SAMPLING OPERATIONS:

Continuous sampling was conducted from the M/V KARA SEAL using the FUGRO Offshore Drilling Rig (FODR). FODR has a three-meter-stroke integral heave compensator that reduces sample disturbance caused by ship motion. In conjunction with rotary drilling used to advance the hole, four sampling devices were used to obtain sediment or rock samples. The devices included: Shelby tubes (thin-walled metal tubes) (Hvorslev, 1949), split barrel samplers (split spoons) (thick-walled metal samplers) (Peck and others, 1974), "O" samplers (split spoon with a liner to better preserve sample integrity), and a Christensen core barrel.

Sample disturbance was reduced by using the sampling device that was most compatible with anticipated sediment behavior at various subbottom depths. Shelby tubes were used in soft material, whereas the split spoon and "O" sampler were used in more competent sediment that would have bent the thin walls of the shelly tube. Although the Christensen core barrel was used in stiffer material, rotary drilling during advancement of the core barrel caused concentric fractures spaced every few centimeters to occur parallel to bedding within the recovered samples.

Except for rotary drilling with the Christensen core barrel, the samplers were driven into the sediment by a hammer. Percussion samples typically are more disturbed than samples obtained with push techniques (Hvorslev, 1949). Emrich (1971) observed a 40 percent decrease in shear strength compared to push samples. However, percussion sampling can indicate relative resistance to penetration by the number of hammer blows required to drive the sampler a fixed distance, typically 0.3 m (Table 2). At least one technique (Bhushan and others, 1976) is available that converts shipboard hammer drops into a blow count analogous to the widely used standard penetration test (SPT) (Peck and others, 1974). The SPT has been used to estimate the compactness or friction angle of granular material and the consistency or undrained shear strength of fine-grained soils (Hunt, 1984).

## SHIPBOARD TESTING METHODS AND RESULTS:

Three devices were used at sea to measure the undrained shear strength of fine-grained sediment: a Torvane, pocket penetrometer, and miniature vane shear machine (Hunt, 1984). Samples for water content (later corrected for a salinity of 35 ppt) were obtained down-hole in coarse-grained material and in fine-grained sediment near strength test locations (Table 2, Figs. 1-4). The undrained shear strengths were determined in finer grained sediment only.

The Torvane has eight small vanes attached to a circular plate; the blades are pushed about 6 mm into a flat sediment surface. The torque required to shear the material at the base of the vanes is measured and related to the undrained shear strength. The Torvane was not used in brittle material where the insertion of the vanes would have fractured the sediment, thereby producing an unrealistically low shear strength.

The pocket penetrometer is operated by pushing a 6-mm-diameter spring-loaded rod 6-mm into a flat sediment surface. The force measured is related to the undrained shear strength. However, the test is only valid for soils with plasticity indices greater than twelve (Hunt, 1984) or shear strengths less than 220 kPa. At many locations the capacity of the device was exceeded (Table 2, Figs. 5-8).

Laboratory miniature-vane tests were performed on the ends of samples, using a 12.6 by 12.6 mm vane, with a rotation rate at the top of the machine's spring of approximately 90 degrees per minute (Lee, in press). The miniature-vane tests were performed to a subbottom depth at which the resistance of the sediment exceeded the allowable torque of the machine's springs. One unconfined compression (UC KS-2) test was performed at sea (Table 4, Fig. 5).

## SAMPLE STORAGE:

Different methods were used to preserve samples for shore-based geotechnical testing depending on the type of sampler used. Wax was poured into the interior of Shelby tubes in order to form a plug against the sediment surface to prevent slumping and dewatering during handling and storage. End caps were then taped onto the ends and dipped in wax. Samples obtained with the Christensen core barrel were cut into approximately 200-mm lengths, wrapped in tin foil, and placed in cardboard tubes. Warm wax was then poured over the sample to completely enclose it. The "O" liner samples were capped and the ends were dipped in wax. All samples were stored on their side at a temperature of approximately four degrees centigrade.

## SHORE-BASED TESTING METHODS AND RESULTS:

Constant rate of strain (CRS) consolidation tests were performed within a triaxial chamber according to the techniques of Wissa and others (1971) in order to evaluate the stress history of the sediment. The test results are plotted as void ratio,  $e$ , versus the logarithm of the vertical effective stress,  $\sigma'_v$  (Appendix A).

Typical  $e - \log \sigma'_v$  curves form a straight line segment, the virgin line, at higher stresses. The slope of the virgin line is termed the compression index,  $C_c$ . The maximum past stress,  $\sigma'_{vm}$ , can be determined from

consolidation test results that have a straight virgin line by Casagrande's (1936) technique. However, most of the consolidation tests performed on Chukchi Sea material did not produce a straight virgin line. That curvature made determination of the maximum past stress highly uncertain (Table 3).

The overconsolidation ratio, OCR, is defined as  $\sigma'_{vm}/\sigma'_{vo}$  where  $\sigma'_{vo}$  is the in-place overburden stress. Sediment with a high OCR typically has experienced a greater amount of preloading than a similar material with a lower overconsolidation ratio at the same overburden stress. The OCRs for the Chukchi Sea material reflect the wide range of values of the maximum past stresses (Table 3). The coefficient of consolidation,  $c_v$ , a factor that reflects the rate at which consolidation occurs, is plotted in Appendix A as a function of the vertical effective stress for each test.

Triaxial tests incorporating the stress history and normalized soil engineering properties (SHANSEP) approach of Ladd and Foott (1974) were planned to estimate the undisturbed in-place shear strength. However, that method relies upon well defined maximum past stresses obtained from consolidation tests. Because consolidation tests typically produced poor results, the SHANSEP approach was not used. Instead, 36-mm-diameter triaxial samples were isotropically consolidated to their estimated in-place vertical effective stress,  $\sigma'_{vo}$ , and sheared undrained using guidelines presented by Bishop and Henkel (1964). The undrained shear strength,  $S_u$  or  $q_{max}$ , was determined as the maximum shear stress attained before 20 percent axial strain was reached (Table 4, Figs. 5-8). The effective friction angle,  $\phi'$ , was determined at the point of maximum obliquity,  $\sigma'_1/\sigma'_3$ , assuming no cohesion intercept (Table 4).

A number of unconfined compression (UC) tests were also performed (according to ASTM Standard D2166-66). They were run in a similar manner to the triaxial tests except that no lateral confinement was given to the samples during testing. Triaxial test and unconfined compression test results are plotted in Appendix B.

#### DISCUSSION:

Based on visual identification, sediment type varies markedly down-hole; sand and gravel are present in some beds whereas only fine-grained sediment exists elsewhere. Geotechnical properties possibly reflect changes in sediment type, as well as, different stress histories for similar sediment types.

Water contents,  $w$ , vary with subbottom depth (Figs. 1-4). In borings 2 and 3 a trend of decreasing water content with depth is apparent, but "spikes" of both higher and lower water content are present. The overall trend of decreasing water content with depth probably results from increasing overburden stresses that cause greater consolidation of the sediment. Borings 4, 7, and 8 show wide variability down-hole. A slight increase in water content with depth is apparent in holes 4 and 7, possibly reflecting down-hole changes in lithology.

Casagrande's (1936) technique for determining  $\sigma'_{vm}$  requires high-quality test results, whereas consolidation testing of the Chukchi Sea samples almost invariably produced poor results (Appendix A). The sharp break in slope

between the reloading and virgin consolidation line apparent in most tests performed on high-quality samples was typically absent. Poorly defined, or nonexistent, straight virgin consolidation lines and difficult to determine points of maximum curvature produced erratic  $\sigma'_{vm}$  determinations (Table 3). The poor results are due to a combination of sample disturbance caused by percussion sampling or rotary drilling and in a few instances result from performing tests on samples with grain sizes that were too coarse to produce well defined consolidation behavior. Some tests may have had such a high maximum past stress that the virgin line was not reached because of equipment limitations.

With few exceptions (CE 137, CE 150, CE 172, and CE 173) the sediment tested appeared overconsolidated (OCR > 1.5, Hunt 1984) to heavily overconsolidated, possibly the result of desiccation caused by low stands of sea-level. The exceptions indicate normal consolidation, i.e., they never experienced a greater vertical effective stress than now exists in situ. The OCR values less than 1.0 are caused by disturbance and hysteretic effects of sampling and testing (Zeevaert, 1983).

Plots of strength values for the various test types versus depth show wide scatter in borings 2 and 3 (Fig. 5). Strengths typically increase with depth, but exceptions occur. Laboratory vane-shear data suggest that an abrupt increase in strength occurs in borings 2 and 3 at a depth of approximately nine meters. However, triaxial tests (TE 257, TE 259) show a gradual increase in strength with depth in that interval. A strong correlation does not exist between different strength-testing methods, although trends are evident. Torvane strengths typically are lower than pocket penetrometer derived values, possibly as a result of remolding soft sediment or fracturing stiff and brittle material.

Triaxial (TE) and unconfined compression (UC) test shear strengths were typically bounded by the pocket penetrometer and torvane values. Relatively good agreement between unconfined strength (UC KS-2, UC 10) and triaxial strength (TE 265, TE 264) was obtained at two locations where the tests were performed on adjacent samples. Considering the size of the tested samples, and operator and equipment inconsistencies associated with shipboard testing, the triaxial and unconfined test results represent the best estimation of in-situ strength. The unconfined compressive strength is probably less than the in-situ strength because of sampling disturbance. The triaxial strength, however, is probably larger than the in-situ strength because consolidation in the laboratory to the in-situ vertical effective stress densifies the material before shear (Ladd and Lambe, 1963, Ladd and Foott, 1974).

Some trends that are evident in holes 2 and 3 also are present in the other borings. However, boring 4 encountered very stiff material within two meters of the seafloor, reflecting the presence of Herald arch. Wide scatter in test results is evident in boring 7.

#### CONCLUSIONS:

Many different sediment types are present on the northern margin of Hope basin and on the southern margin of the North Chukchi basin. The varying material types may be responsible for observed non-uniform geotechnical behavior down-core. Typically water contents decrease and strength increases

with depth in borings 2 and 3 located in the North Chukchi basin. Water content and strength determinations are more erratic in the other borings.

Consolidation test results were very poor because of sample disturbance caused by percussion sampling and the presence of clay-lacking grain-sizes. Percussion sampling produces extensive disturbance; therefore, in order to obtain more meaningful geotechnical data push sampling methods should be used whenever possible in future operations.

Pocket penetrometer strength values were typically higher than triaxial and unconfined compression values, and torvane test strengths were the lowest. Triaxial and unconfined compression tests probably produced values closest to the in-situ strengths.

#### ACKNOWLEDGEMENTS:

The authors wish to thank the reviewers of this report, R.E. Hunter and D.A. Dinter, for their helpful comments and suggestions. R.E. Kayen performed most of the shore-based laboratory testing. P.A. Swenson drafted the figures.

## REFERENCES:

- Bhushan, K., Mahmood, A., and Allen, R.L., 1976, Resistance of ocean sediments to sampler penetration. Eighth Offshore Technology Conference, paper no. 2624, p. 55-64.
- Bishop, A.W. and Henkel, D.J., 1964, The Measurement of Soil Properties in the Triaxial Test. London, Edward Arnold, Ltd. (Publishers), 227 p.
- Casagrande, A., 1936, The determination of the pre-consolidation load and its practical significance. Proceedings First International Conference on Soil Mechanics and Foundation Engineering, v. 3, Cambridge, Massachusetts, p. 60-64.
- Emrich, W.J., 1971, Performance study of soil sampler for deep-penetration marine borings. In: Sampling of Soil and Rock, American Society for Testing and Materials Special Technical Publication 483, p. 30-50.
- Grantz, A., Holmes, M.L., and Kososki, B.A., 1975, Geologic framework of the Alaskan continental terrace in the Chukchi and Beaufort Seas. In: Yorath, C.J., Parker, E.R., and Glass, D.J. (eds.), Canada's Continental Margins and Offshore Petroleum Exploration. Canadian Society of Petroleum Geologists, Calgary, Canada, p. 669-700.
- Holmes, M.L. and Creager, J.S., 1981, The role of the Kaltag and Kobuk faults in the tectonic evolution of the Bering Strait region. In: Hood, D.W. and Calder, J.A. (eds.), The Eastern Bering Sea Shelf: Oceanography and Resources, v. 1. U.S. Dept. of Commerce, National Oceanic and Atmospheric Administration, p. 293-302.
- Hunt, R.E., 1984, Geotechnical Engineering Investigation Manual. New York, McGraw-Hill Book Company, 983 p.
- Hvorslev, M.J., 1949, Subsurface Exploration and Sampling of Soils for Civil Engineering Purposes. The Engineering Foundation, New York, 521 p.
- Ladd, C.C. and Foott, R., 1974, New design procedures for stability of soft clays. Journal of the Geotechnical Engineering Division, ASCE, July, p. 763-786.
- Ladd, C.C. and Lambe, T.W., 1963, The strength of undisturbed clay determined from undrained tests. Laboratory Shear Testing of Soils, American Society for Testing and Materials Special Technical Publication 361, p. 342-371.
- Lee, H.J., in press, State of the art: laboratory determination of the strength of marine soils. American Society for Testing and Materials Special Technical Publication. Proceedings of the Symposium on Laboratory and In Situ Determination of the Strength of Marine Soils.
- Peck, R.B., Hanson, W.E., and Thornburn, T.H., 1974, Foundation Engineering, New York, Wiley, 514 p.

Wissa, A.E., Christian, J.T., Davis, E.H., and Heiberg, S., 1971,  
Consolidation at constant rate of strain. Journal of the Soil Mechanics  
and Foundations Division, ASCE, October, p. 1393-1413.

Zeevaert, L., 1983, Foundation Engineering for Difficult Subsoil Conditions.  
New York, Van Nostrand Reinhold Company, 676 p.

## NOMENCLATURE AND SYMBOLS:

- ASTM - American Society for Testing and Materials.
- C - Christensen core barrel sampler.
- $C_c$  - Compression index, defined as the slope of the linear part of a consolidation curve plotted on a graph of void ratio versus log of effective stress.
- CE - The prefix for a constant rate of strain (CRS) consolidation test number.
- cm - Centimeter.
- $c_v$  - Coefficient of consolidation, a factor that reflects the rate at which consolidation occurs.
- $c_{v \text{ ave}}$  - The average of coefficients of consolidation for a consolidation test.
- DELTA u - The change in excess pore water pressure from the beginning of a shear test.
- Dev Stress - The deviator stress or difference between the major and minor principal effective stresses ( $\sigma'_1 - \sigma'_3$ ).
- e - Void ratio, defined as the volume of voids divided by the volume of solids.
- km - Kilometer.
- kPa - KiloPascal,  $\text{kN/m}^2$ .
- m - Meter
- mm - Millimeter.
- "O" - Split spoon sampler with a liner.
- OCR - Overconsolidation ratio, ( $\sigma'_{vm}/\sigma'_{vo}$ ).
- OE - Prefix for an oedometer test number.
- ppt - Part per thousand.
- $p'$  - The normal effective stress acting on a plane inclined at 45 degrees from the horizontal in a triaxial test  $(\sigma'_1 + \sigma'_3)/2$ .
- $q$  - The shear stress acting on a plane inclined at 45 degrees from the horizontal in a triaxial test  $(\sigma'_1 - \sigma'_3)/2$ .
- $q_{\text{max}}$  - Maximum value of  $q$  reached during a static triaxial test, equal to  $S_u$ .
- S - Shelby tube sampler (thin-walled).
- SHANSEP - Stress history and normalized soil engineering properties (an approach to estimating in-situ shear strength by extrapolating laboratory tests to field conditions).
- SPT - Standard penetration test.
- $S_r$  - Remolded undrained shear strength.
- SS - Split spoon sampler (thick walled).
- $S_t$  - Sensitivity ( $S_u/S_r$ ).
- SIG  $1_c'$  - The major (or vertical) principal stress applied to a triaxial test sample prior to shear.
- SIG  $3_c'$  - The minor (or horizontal) principal stress applied to a triaxial test sample prior to shear.
- $S_u$  - Undrained shear strength.
- TE - Prefix for a static triaxial test number.
- UC - Prefix for an unconfined compression shear test.
- w - Water content (weight of water including salt/weight of solids).
- $\sigma'_1$  - The major (or vertical) principal effective stress applied to a triaxial test sample.
- $\sigma'_1/\sigma'_3$  - obliquity factor; it is a maximum at the point of the largest friction angle during a triaxial test.
- $\sigma'_3$  - The minor (or horizontal) principal effective stress applied to a triaxial test sample.

- $\sigma'_c$  - The consolidation stress exerted on a triaxial test sample prior to shear.
- $\sigma'_v = \sigma'_{v0}$  - The in-situ vertical effective stress exerted by the weight of overburden.
- $\sigma'_{vm}$  - The maximum vertical effective stress that a sediment has ever experienced.
- $\phi'$  - The friction angle of a sediment expressed in terms of effective stresses.

Table 1. Station Locations.

Boring	Latitude	Longitude	Water Depth (m)	Location
2*	70°40.014'N	167°19.594'W	53.9	Southern margin of North Chukchi Basin
3*	70°40.014'N	167°19.594'W	53.9	Southern margin of North Chukchi Basin
4	70°27.676'N	167°05.205'W	51.2	Northern flank of Herald Arch
5	69°59.146'N	168°04.943'W	48.5	On Herald Arch
6	69°50.506'N	168°22.205'W	47.0	On Herald Arch
7**	69°37.901'N	168°51.785'W	49.4	Extreme Northern margin of Hope Basin
8**	69°37.911'N	168°51.776'W	53.0	Extreme Northern margin of Hope Basin

\* Borings 2 and 3 are spaced approximately 7 meters apart.

\*\* Borings 7 and 8 are spaced approximately 7 meters apart.

Table 2. Boring Information, Shipboard Strength Test Results, and Water Contents.

Boring No.	Section No.	Depth To Section Top (m)	Sampler Type	Hammer Blows/0.3m	Test Depth (m)	Water Content (%)	S <sub>u</sub> lab vane (kPa)	S <sub>r</sub> lab vane (kPa)	S <sub>t</sub>	S <sub>u</sub> Torvane (kPa)	S <sub>u</sub> pocket pen. (kPa)
2	1	0.4	S		0.6	24.4				7	37
3	1	0.0	S		0.6	53.8	7.6	2.3	3.3	5	
2	2	0.6	S		1.2	52.6	3.1				
	3	1.2	S		2.1	32.4	0.4				20
	4	2.1	S		2.7	27.6					
	5	2.7	S		3.4	27.6	24				
	6	3.4	S		4.0	31.4	23				
	7	4.0	S		4.6	25.7	14				
	8	4.6	S		5.2	27.1	6.4				
	9	5.2	S		5.8	23.3					
3	2	5.2	S	12	5.8	32.5	2.8	2.0	1.4		
	3	5.8	S	10	6.4	26.0					
	4	6.4	S	17	7.0	25.6					
	5	7.0	S	17	7.6	37.7					
	6	7.6	S	20	8.2	24.1					
	7	8.2	S	25	8.8	30.7	14	3.2	4.4		
	8	8.8	S	27	9.4	25.3					
	9	9.4	S	25	10.0	28.9					
	10	10.1	S	30	10.6	13.8					
	11	10.7	S	30	11.3	19.1	200	49	4.0	120	190
	12	11.3	S	30	11.9	14.1				91	180
	13	11.9	S	37	12.5	24.8					>220
	14	12.5	S	37	13.1	24.9					>220
	15	13.1	S	40	13.7	25.7					>220
	16	13.7	S	35	14.3	22.6					>220
	17	14.3	C		15.0	38.8					74
	18	15.2	C		16.2					86	170
	19	16.2	C		17.6	25.4				74	>220
	20	17.7	C		19.2	25.3				54	120
	21	19.2	C		19.4	22.5					>220
	22	20.1	C		20.4	26.9					170
	23	21.6	C		22.0	19.8					>220
	24	22.6	C		23.2	22.6					>220
	25	23.5	C		24.6	23.2					>220

Table 2. continued

Boring	Section No.	Depth To Section Top (m)	Sampler Type	Hammer Blows/0.3m	Test Depth (m)	Water Content (%)	S <sub>u</sub> lab vane (kPa)	S <sub>r</sub> lab vane (kPa)	S <sub>t</sub>	S <sub>u</sub> Torvane (kPa)	S <sub>u</sub> pocket pen. (kPa)
	26	24.7	C		24.8	20.3					>220
	27	25.5	C		25.7	16.8					>220
	28	26.5	C		27.7	37.7					>220
	29	27.7	C								
	30	29.3	C		30.4	24.4					210
	31	30.8	C		31.6	24.3					
	32	32.3	C		32.7	48.3					
	33	33.5	C		34.9	22.7					>220
	34	35.4	C		36.4	19.8					>220
	35	36.9	C		37.3	20.7					>220
	36	38.4	C		39.3	20.7					>220
	37	39.9	C		40.1	19.2					>220
	38	41.5	C		42.8	21.4			100		>220
	39	43.0	C		44.3	43.7			110		>220
	40	44.5	C		45.6	18.0			>49(b)		>220
	41	46.0	C		47.2	17.5					>220
	42	47.5	C		47.3	18.8					>220
	43	49.1	C		49.7	19.5					220
	44	50.0	S		51.3	13.9					220
4	1	0.0	S	1	0.1	20.8	116			36	170
	2	0.6	S	2	1.2	23.9	58			22	80
	3	1.2	S	5	1.8	19.1	185			54	210
	4	1.8	S	10	2.7	18.7					220
	5	2.7	SS	15	2.9	20.0					
	6	4.0	C		4.5	20.4					>220
	7	5.2	C		5.6	22.5					>220
5	1	0.0	S	10	0.6	11.4					
	2	0.6	S	20	1.2	12.8					
	3	1.2	SS	50	1.5						
	4	1.5	SS	100	1.7						
	5	1.7	SS	120	1.8						
	6	1.8	SS	100(?)	2.4						
	7	2.4	SS	100(?)	2.7						
6	1	0.0	S	10	0.2	53.4					
	2	0.2	SS	20	0.2						
	3	0.6	SS	80	0.6						
	4	0.8	SS	100	0.8						
	5	0.9	SS	75	0.9						

Table 2. continued

Boring	Section No.	Depth To Section Top (m)	Sampler Type	Hammer Blows/0.3m	Test Depth (m)	Water Content (%)	S <sub>u</sub> lab vane (kPa)	S <sub>r</sub> lab vane (kPa)	S <sub>t</sub>	S <sub>u</sub> Torvane (kPa)	S <sub>u</sub> pocket pen. (kPa)
7	1	0.0	S	1	0.6	14.0	>200			49	>220
	2	0.6	S	17	1.2	16.8				70	130
	3	1.2	S	17	1.8	17.3				76	120
	4	1.8	SS	10	2.4	23.1					
	5	1.8	S	20	2.4	24.0					
	6	2.4	O	20	3.0	21.8					150
	7	3.0	S	15	3.7	18.9					
	8	3.7	O	20	4.3	13.2			130		
	9	4.3	O	20	4.9	18.9			56		
	10	4.9	O	20	5.5	17.1					>220
	11	5.5	O	20	6.0	17.5					>220
	12	6.1	O	25	6.7	28.3					37
	13	6.7	S	15	7.3	21.7					51
	14	7.3	O	20	7.9	17.0					>220
	15	7.6	O	20	8.5	19.4					86
	16	7.9	S	25	8.5						
	17	8.5	O	25	9.1	13.7					98
	18	9.1	O	25	9.8	11.5					>220
	19	9.8	O	25	10.4	16.1					>220
	20	10.4	SS	20	11.0	17.8					
	21	11.0	O	15	11.6	19.2					>220
	22	11.6	O	15	12.0	26.9					
	23	12.2	O	15	12.8	15.3					>220
	24	12.8	O	15	13.4	24.1					>220
	25	13.4	O	15	14.0	26.6					>220
	26	14.0	O	15	14.6	24.3					150
	27	14.6	O	15	15.2						
	28	15.2	O	15	15.3	18.0					220
8	1	0.0	O	20	0.5	30.7				29	120
	2	0.6	O	25	1.2	13.9				61	>220
	3	1.2	O	20	1.8	21.1				39	127
	4	1.8	O	20	2.4	23.6				37	86
	5	2.4	O	25	3.0	15.8				12	98
	6	3.0	O	30	3.6	17.5				2	10

(a) Water content was corrected for a pore water salinity of 35 ppt.

(b) Insertion of Torvane fractured stiff sediment.

Table 3. Consolidation Test Results.

Boring	Section No.	Test Depth (m)	Initial Water Content (%)	Consolidation Test No.	$q'_{VO}$ (kPa)	$\sigma'_{vm}$ (kPa)	OCR $\left(\frac{\sigma'_{vm}}{\sigma'_{VO}}\right)$	$C_c$	$c_v$ (ave) (cm <sup>2</sup> /sec)
2	2	1.0	48.6	CE137	8	8	1	0.25	$2 \times 10^{-3}$
	6	3.7	27.2	CE140	33	2000 (?)	61	0.16	$3 \times 10^{-1}$
	6	3.7	27.7	CE149	33	950 (?)	29	0.18	--
	8	4.9	26.9	CE132	45	450 (?)	10	0.24	$1 \times 10^{-2}$
	8	4.9	26.9	CE133	45	3800 (?)	84	0.05	--
	2	5.5	25.4	CE136	50	1200 (?)	24	0.06	$3 \times 10^{-1}$
	11	11.0	23.1	CE141	106	300	2.8	0.24	$2 \times 10^{-1}$
	14	12.8	25.1	CE134	120	700 (?)	5.7	0.25	$1 \times 10^{-3}$
3	14	12.8	25.1	CE135	120	300 (?)	2.4	0.17	$3 \times 10^{-3}$
	19B	16.5	23.0	CE167	160	420 (?)	2.6	0.17	$5 \times 10^{-3}$
	28F	26.7	26.6	CE168	260	1100 (?)	4.2	0.05	$2 \times 10^{-3}$
	33I	35.0	25.4	CE150	340	250	0.7	0.12	$9 \times 10^{-4}$
	38H	42.7	24.8	CE172	410	160	0.4	0.15	$2 \times 10^{-3}$
	43E	49.7	20.5	CE173	470	450	1.0	0.35	$1 \times 10^{-3}$
	1	0.3	12.9	CE146	3.7	2500 (?)	680	0.13	$4 \times 10^{-1}$
	21	11.3	19.1	CE147	130	310 (?)	2.4	0.16	$1 \times 10^{-1}$
7	24	13.2	27.9	CE148	150	2500 (?)	17	0.32	--
	1	0.1	30.0	CE174	1	480 (?)	480	0.11	$1 \times 10^0$

Table 4. Triaxial and Unconfined Compression Test Results

Boring	Section No.	Test Depth (m)	Initial Water Content (%)	Strength Test No.	Water Content After Shear (%)	Strain to Failure (%)	$S_u$ (kPa)	$\phi'$ (degrees)	$\sigma'_c$ (kPa)	$S_u / \sigma'_c$
2	2	1.1	50.0	TE258	44.5	20.0	11.6	43.5	6.2	1.9
	6	3.6	29.6	TE257	24.8	19.9	58.5	39.0	29.7	2.0
3	2	5.6	23.9	TE259	27.8	4.6	134	41.6	39.3	3.4
	14	13.0	23.7	TE260	26.8	7.7	167	35.1	109.7	1.5
7	18	16.2	--	UC KS-2	--	12.8	135	--	--	--
	19B	16.5	29.3	TE265	25.0	18.6	153	33.4	160	0.95
8	28F	26.7	22.4	TE266	23.0	17.3	278	33.7	209	1.3
	33I	35.1	23.9	TE264	27.1	3.7	224	29.7	330	0.68
7	33I	35.2	22.0	UC10	22.0	6.4	199	--	--	--
	38H	42.7	24.8	TE270	24.7	8.8	173	45.5	406	0.42
7	43E	49.6	23.8	TE271	22.4	6.4	308	24.3	477	0.65
	1	0.5	11.9	TE261	14.8	11.1	55.1	42.2	4.2	--
21	21	11.5	19.8	TE262	14.6	5.1	463	40.4	123	3.8
	24	13.3	26.6	TE263	25.3	19.4	180	34.4	144	1.2
8	1	0.1	34.6	TE269	27.2	19.9	9.4	45.8	1.0	--
	4	2.2	29.0	TE225	28.7	18.7	50.9	40.9	19.9	2.6
6	6	3.4	17.2	TE226	16.4	9.2	177	36.5	34.7	5.1

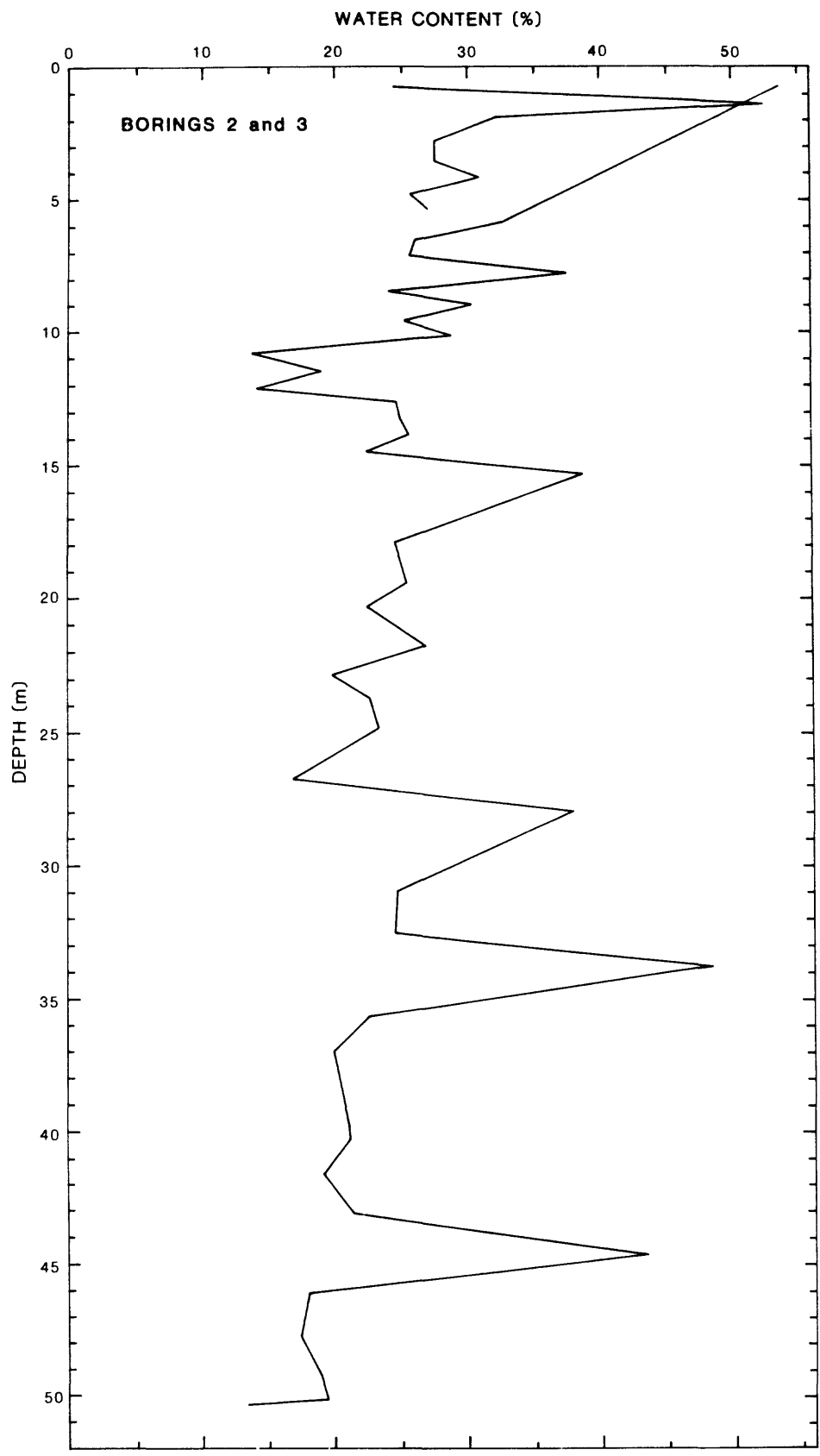


Fig. 1. Water content versus subbottom depth from borings 2 and 3.

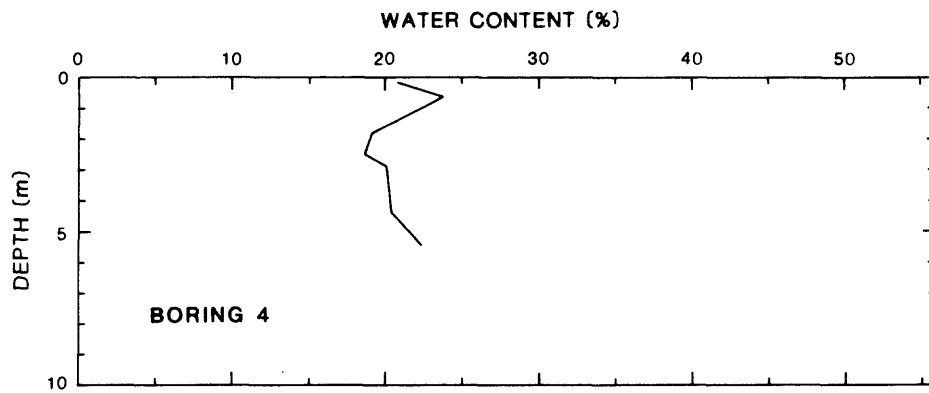


Fig. 2. Water content versus subbottom depth from boring 4.

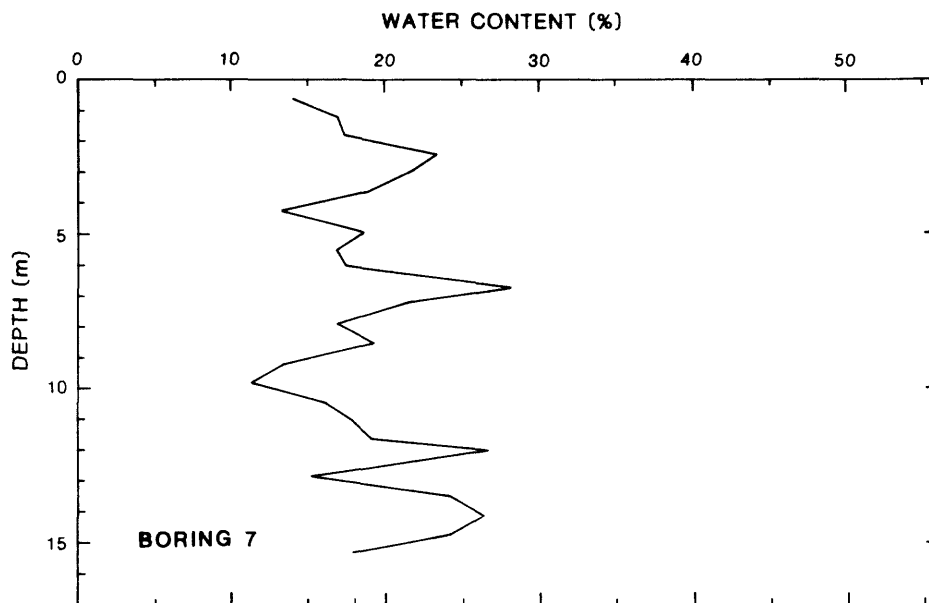


Fig. 3. Water content versus subbottom depth from boring 7.

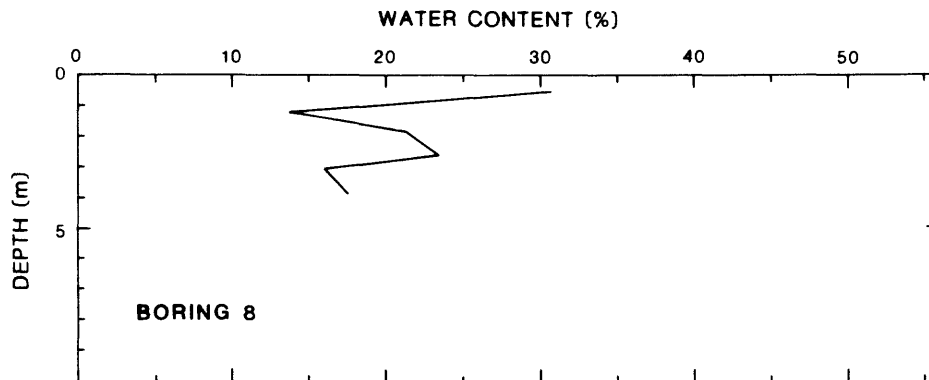


Fig. 4. Water content versus subbottom depth from boring 8.

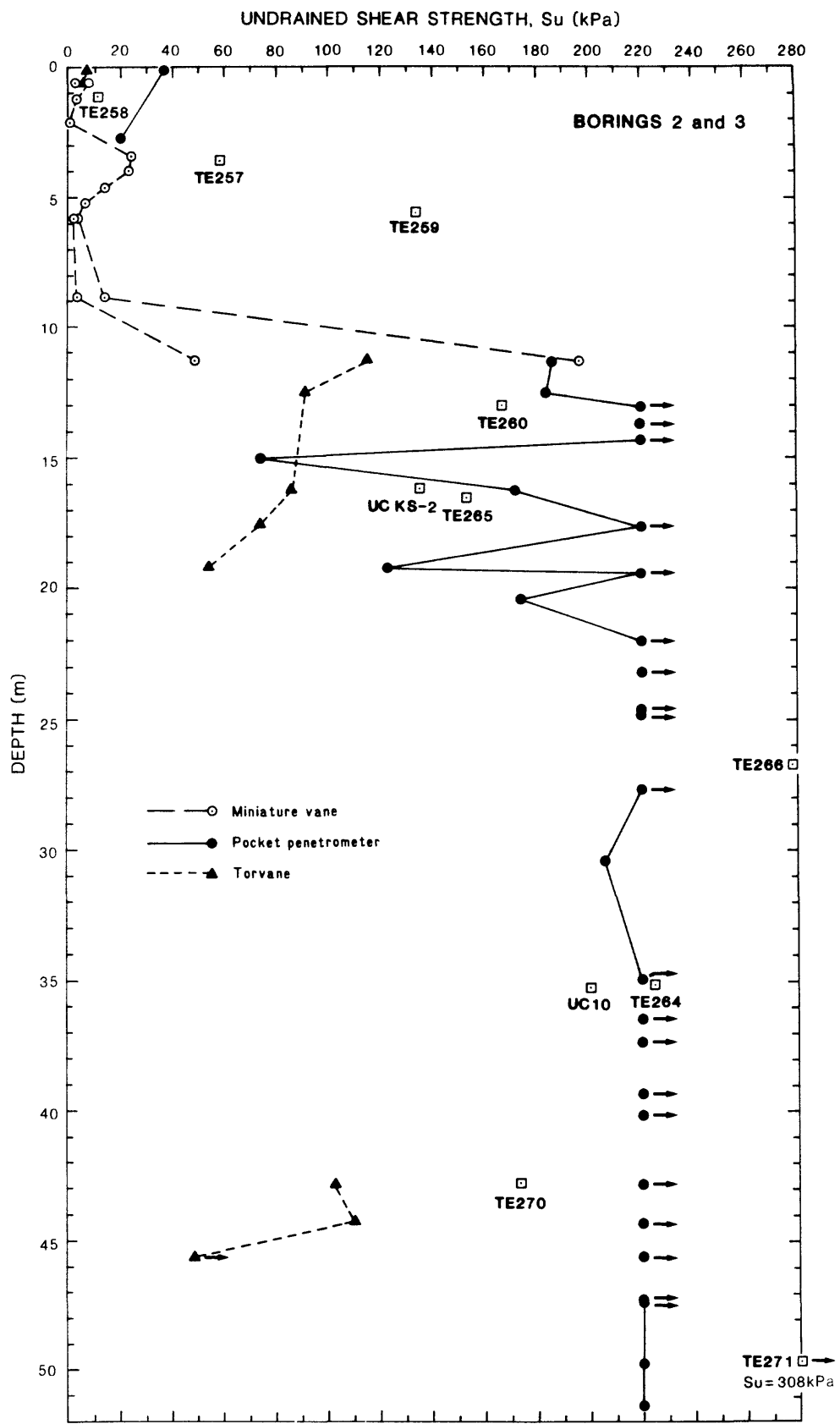


Fig. 5. Undrained shear strength,  $S_u$ , versus subbottom depth from borings 2 and 3.

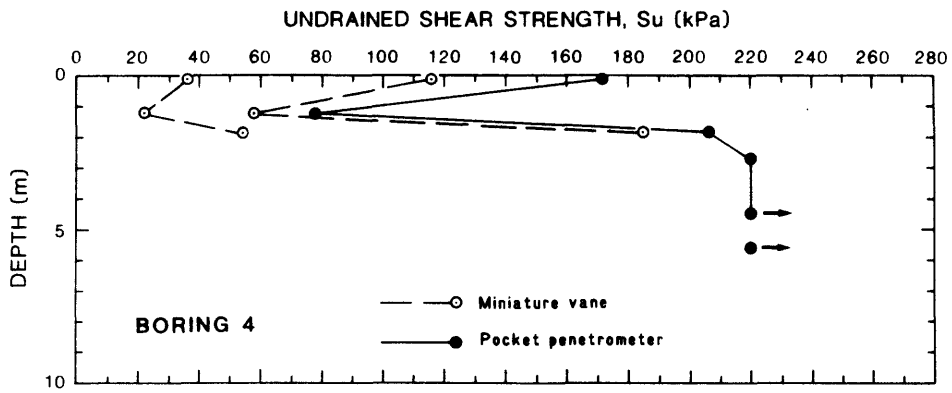


Fig. 6. Undrained shear strength,  $S_u$ , versus subbottom depth from boring 4.

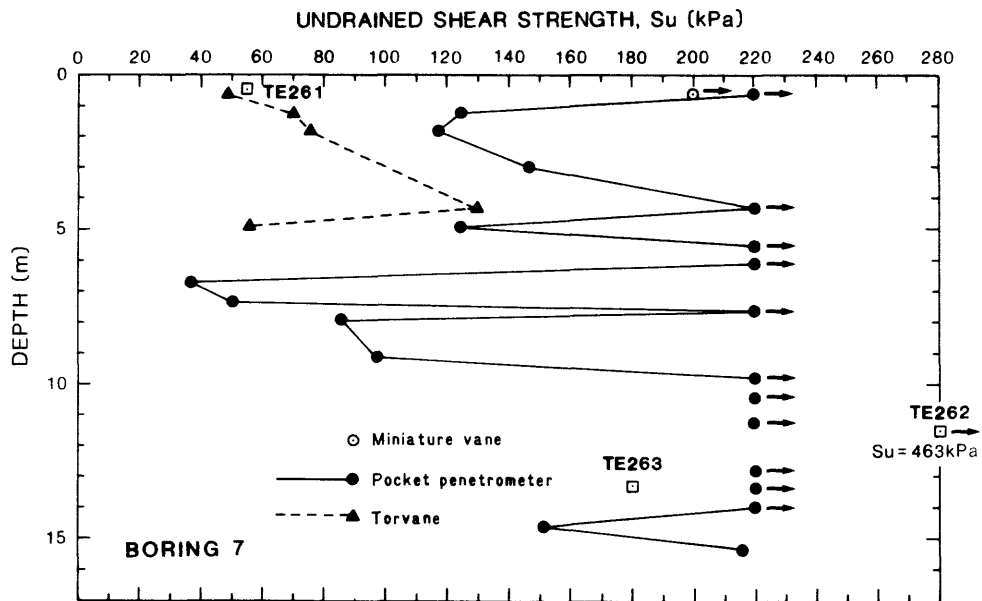


Fig. 7. Undrained shear strength,  $S_u$ , versus subbottom depth from boring 7.

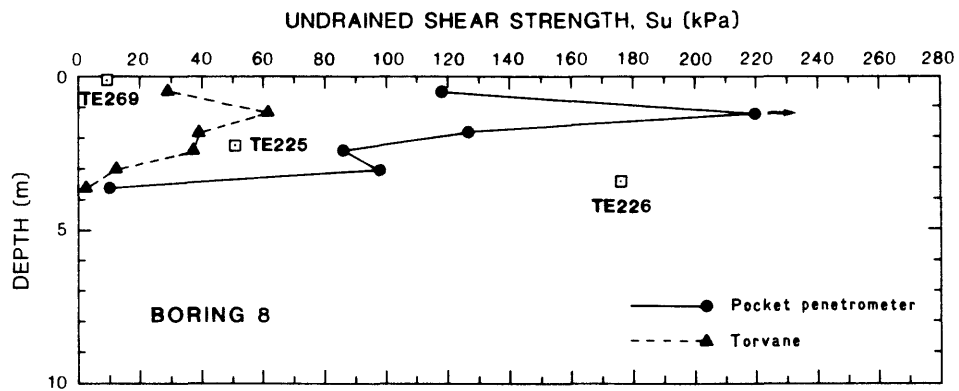
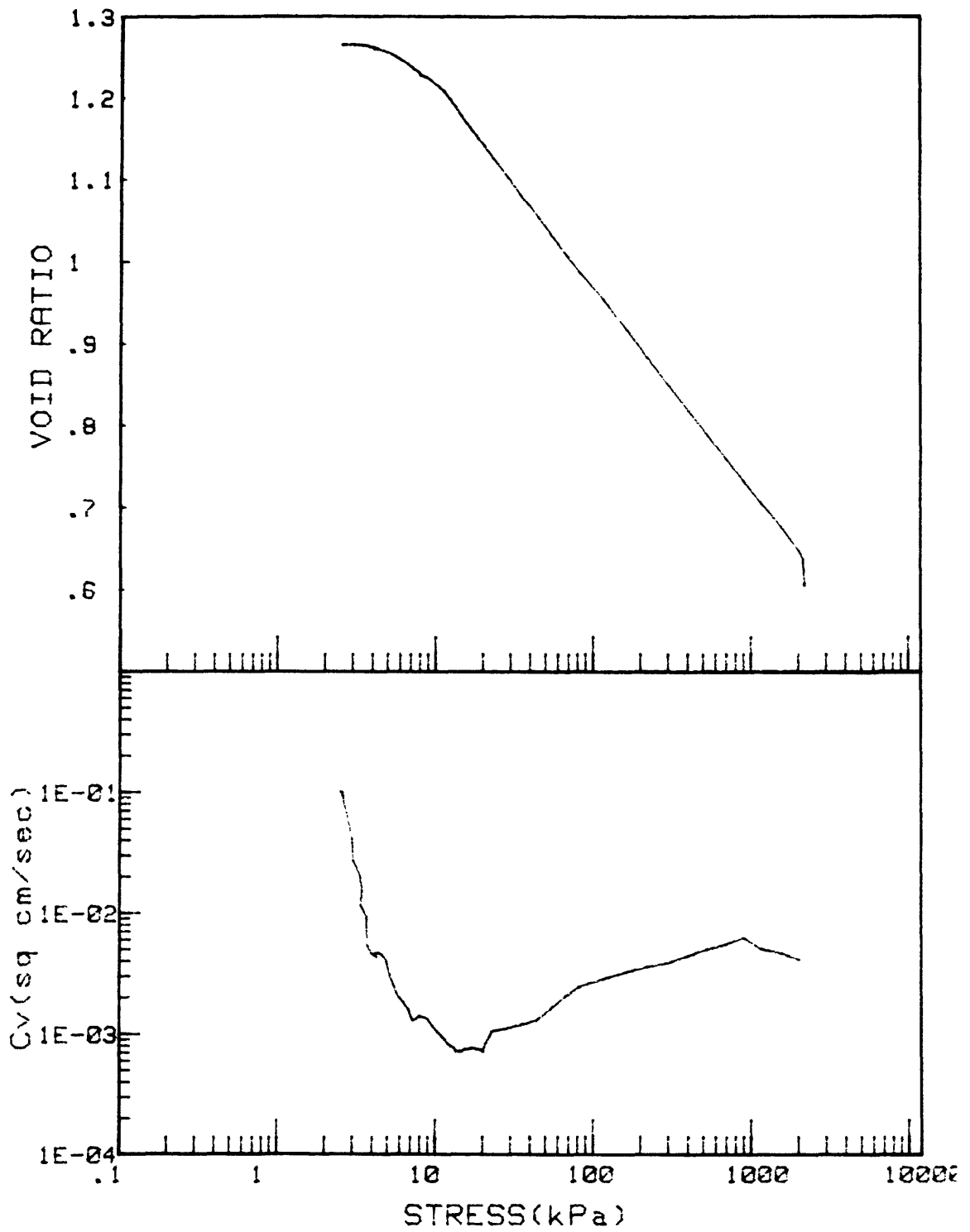


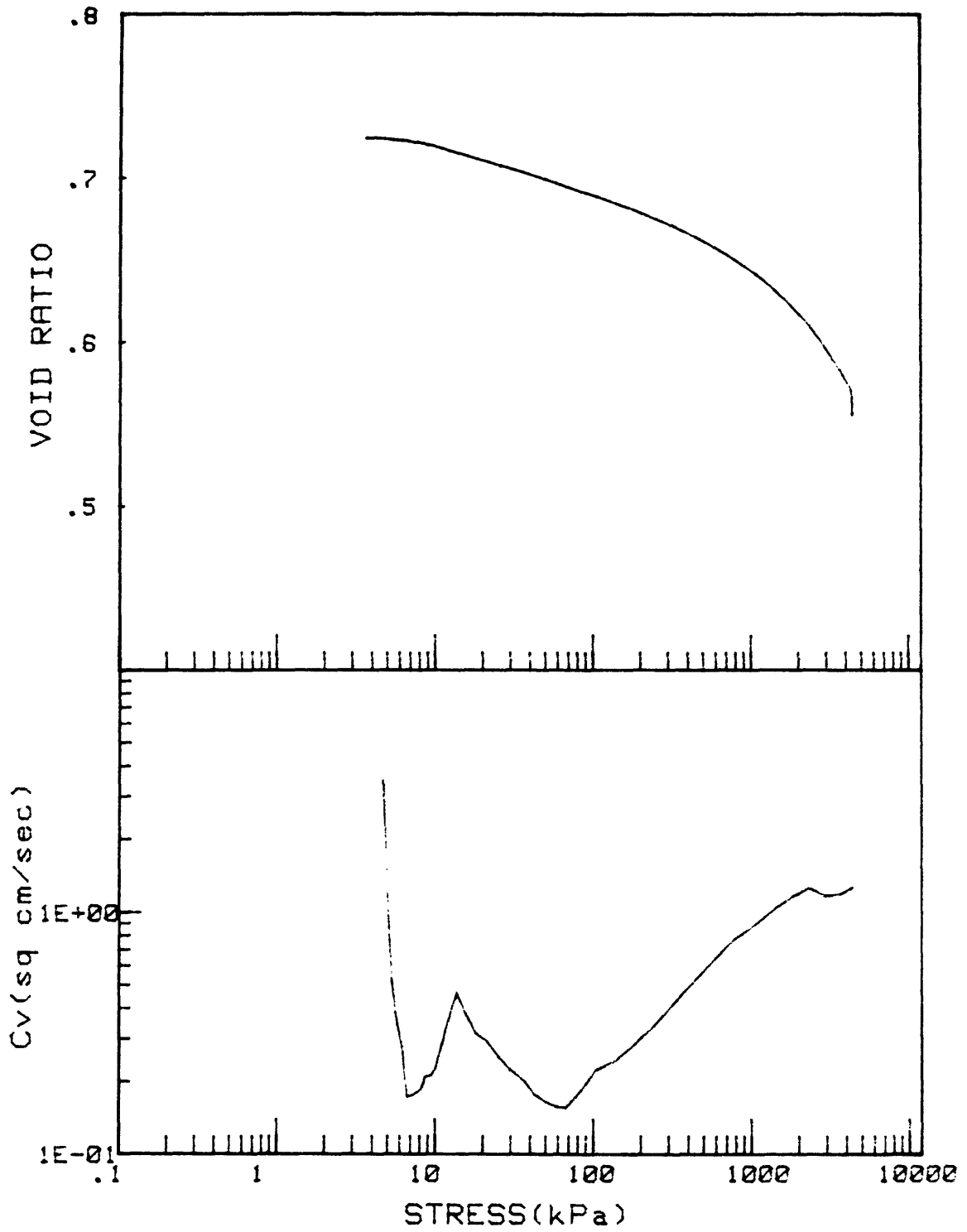
Fig. 8. Undrained shear strength,  $S_u$ , versus subbottom depth from boring 8.

APPENDIX A

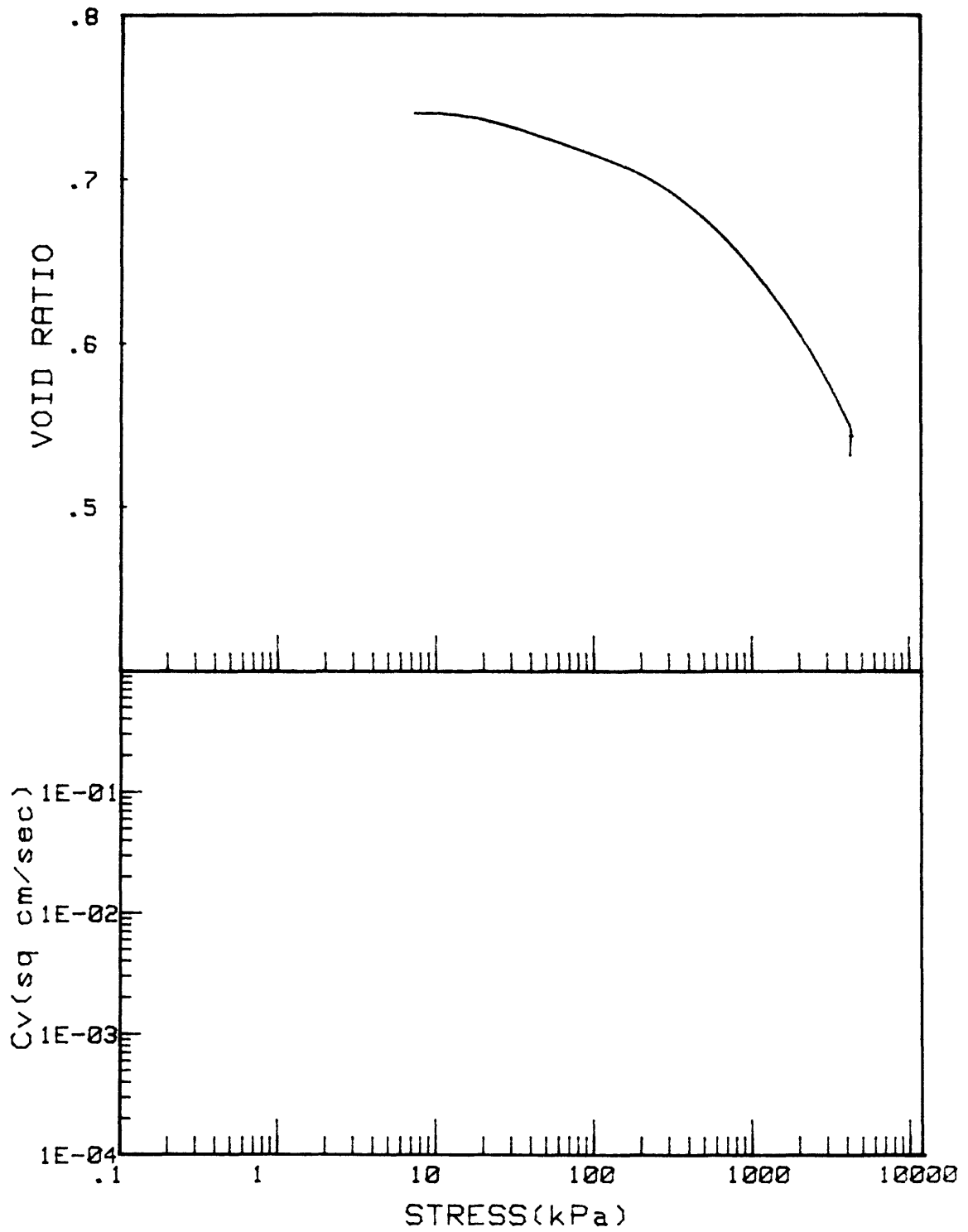
CONSOLIDATION TEST RESULTS



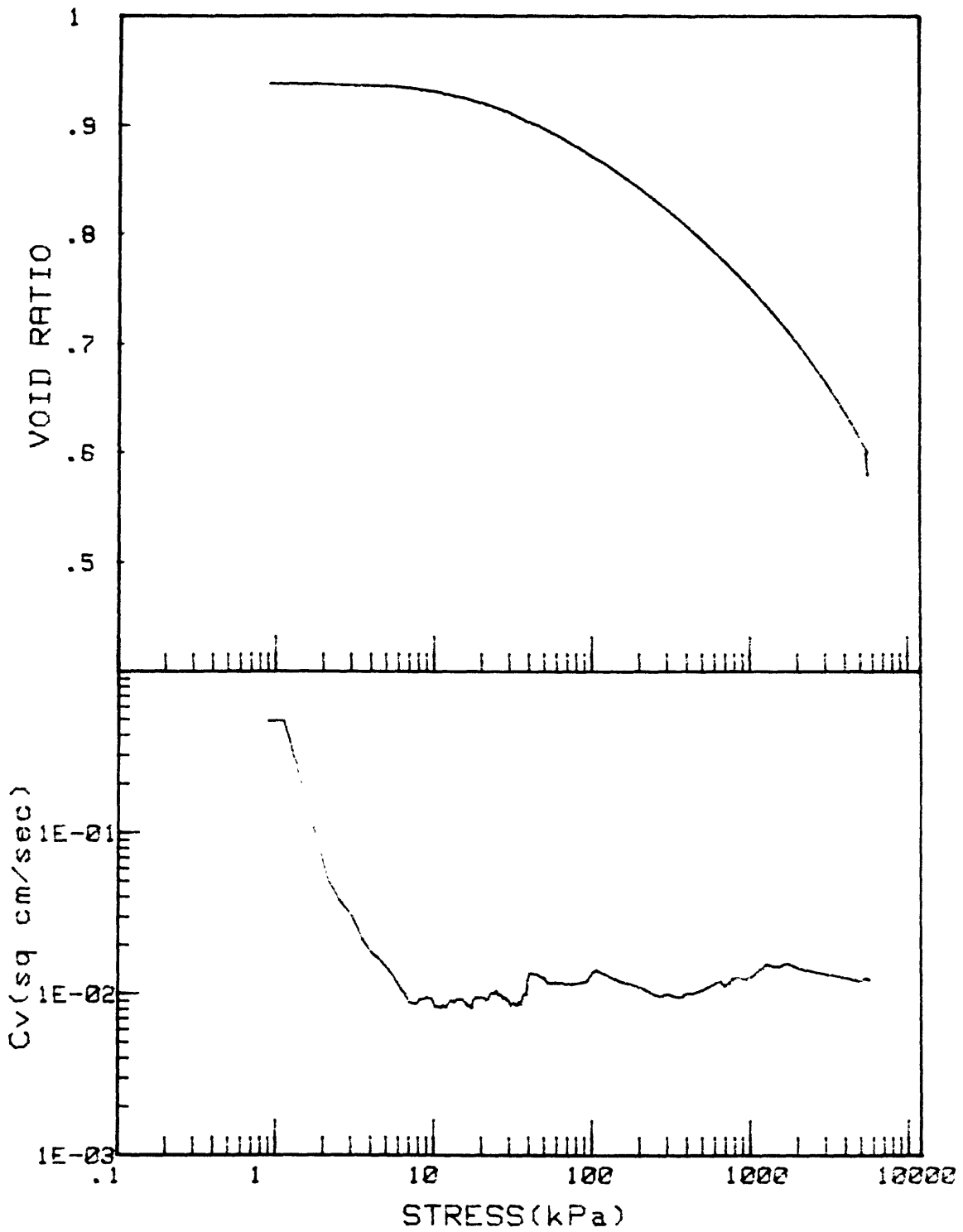
KS1-83-CS	INCREMENT (cm)	SECTION 2
CORE NO.	BORING 2 TEST NO.	CE137



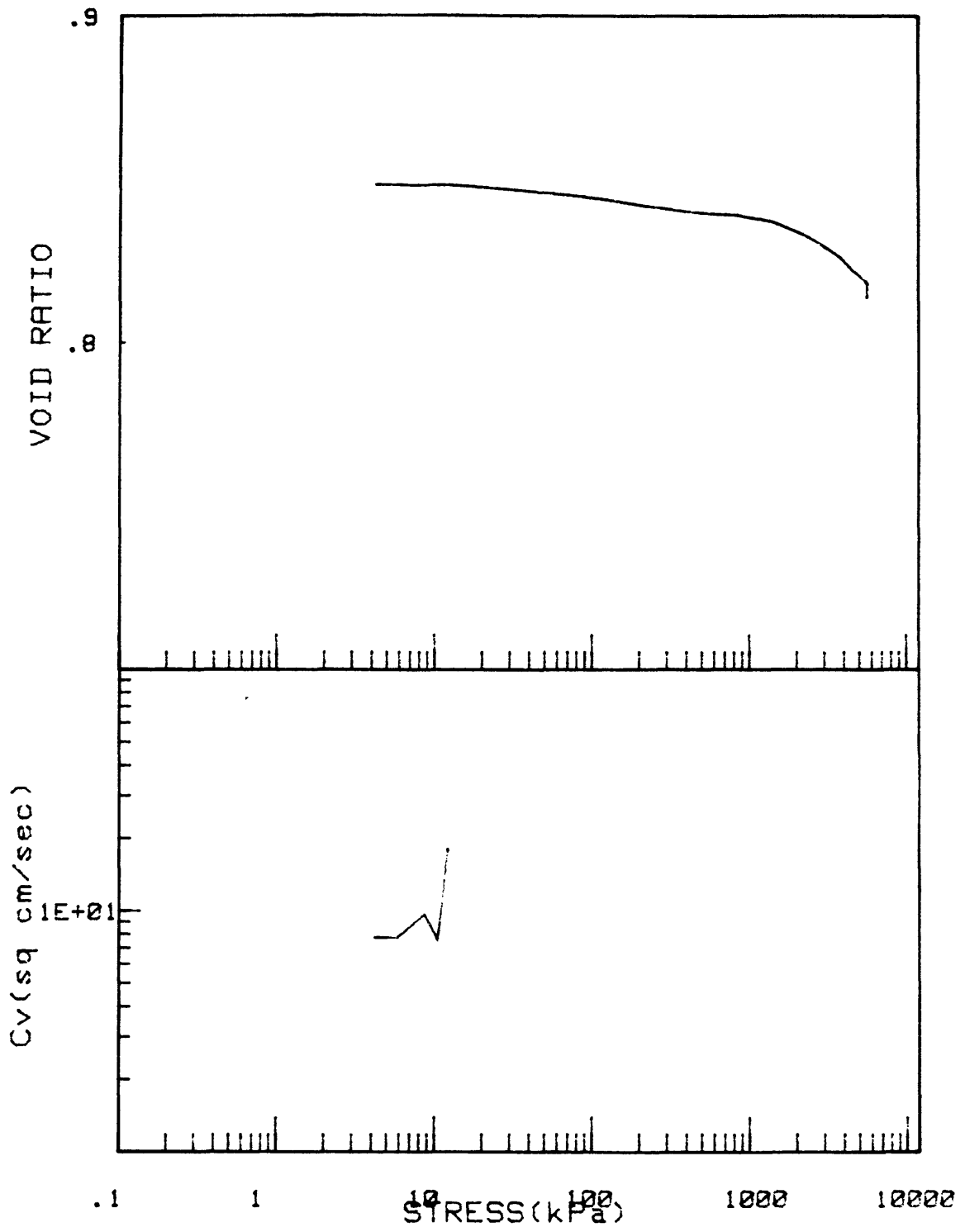
KS1-83-CS	INCREMENT (cm)	SECTION 6
CORE NO.	BORING 2 TEST NO.	CE140



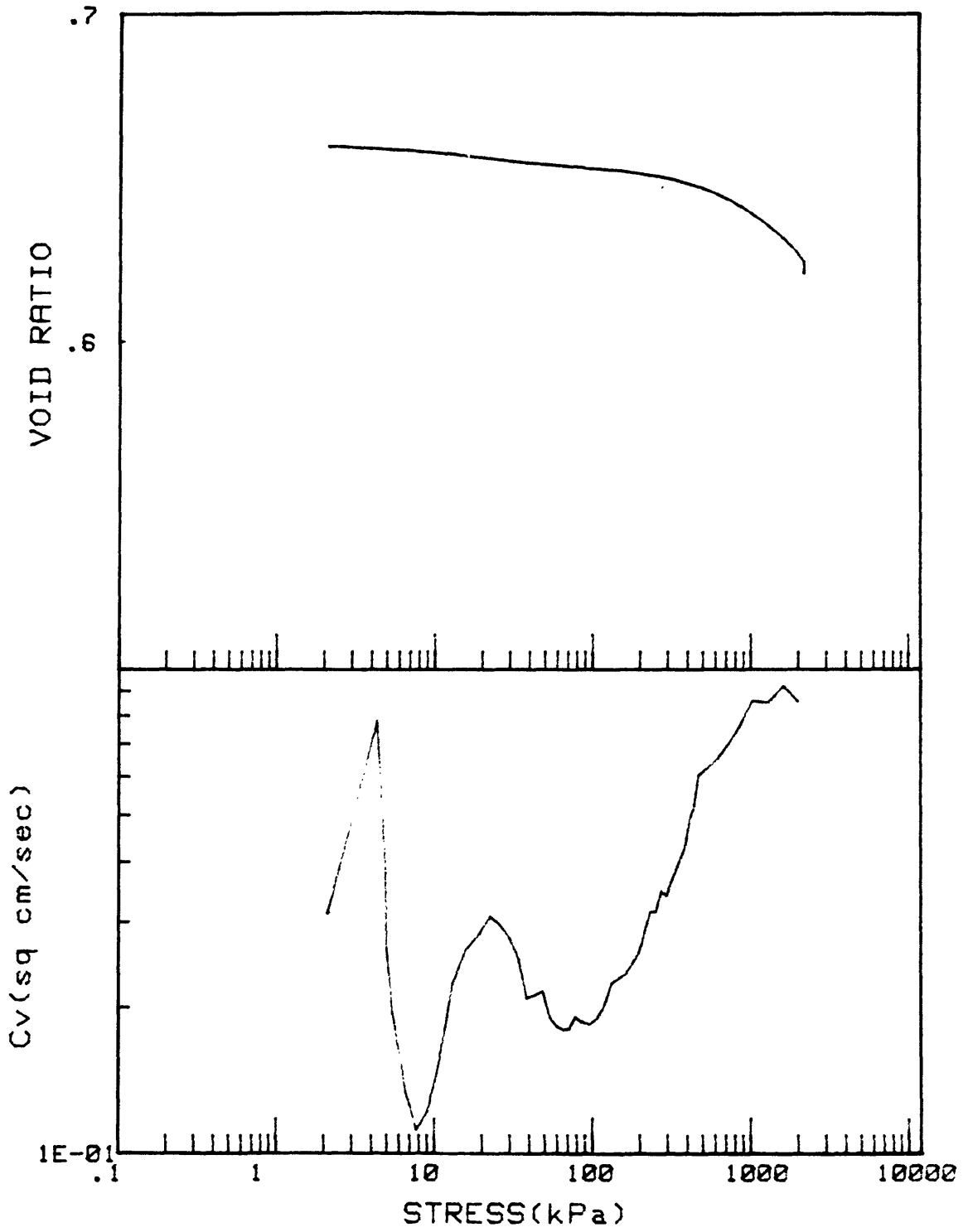
KSI-83-CS		INCREMENT (cm)	S-6
CORE NO. B-2		TEST NO.	CE149



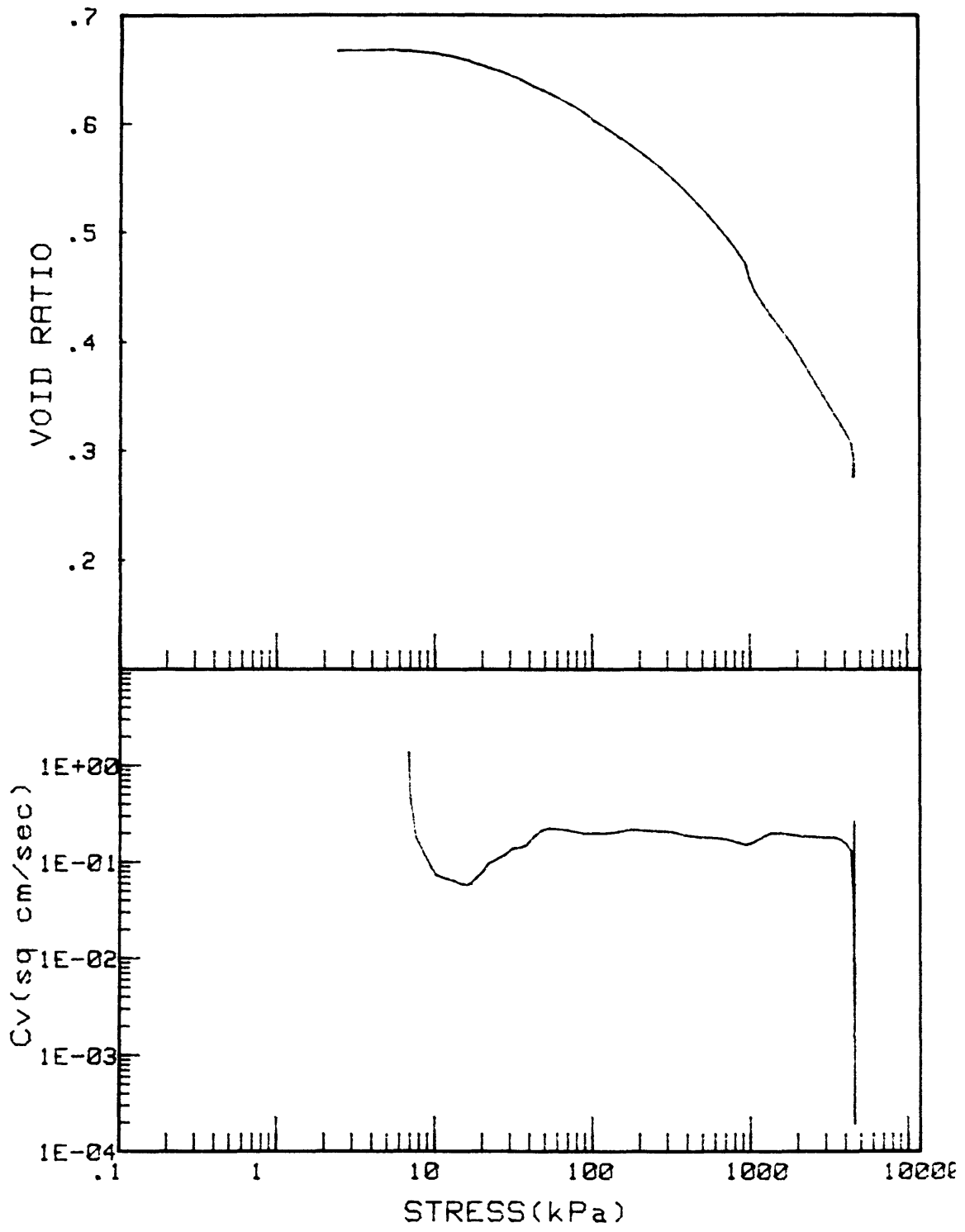
KSI-83-CS	INCREMENT (cm)	SECTION 8
CORE NO.	BORING 2 TEST NO.	CE132



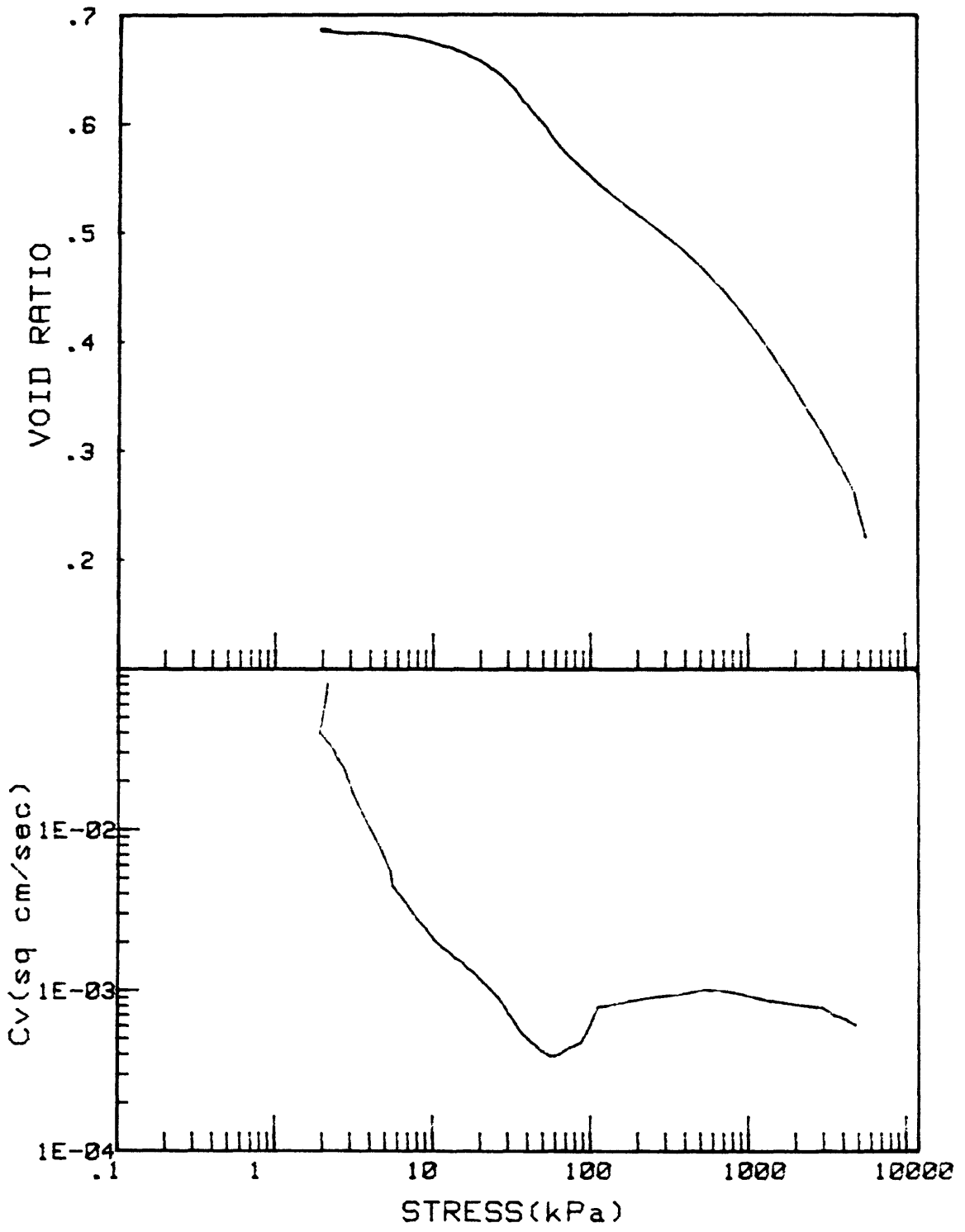
KS1-83-CS	INCREMENT (cm)	SECTION 8
CORE NO.	BORING 2 TEST NO.	CE133



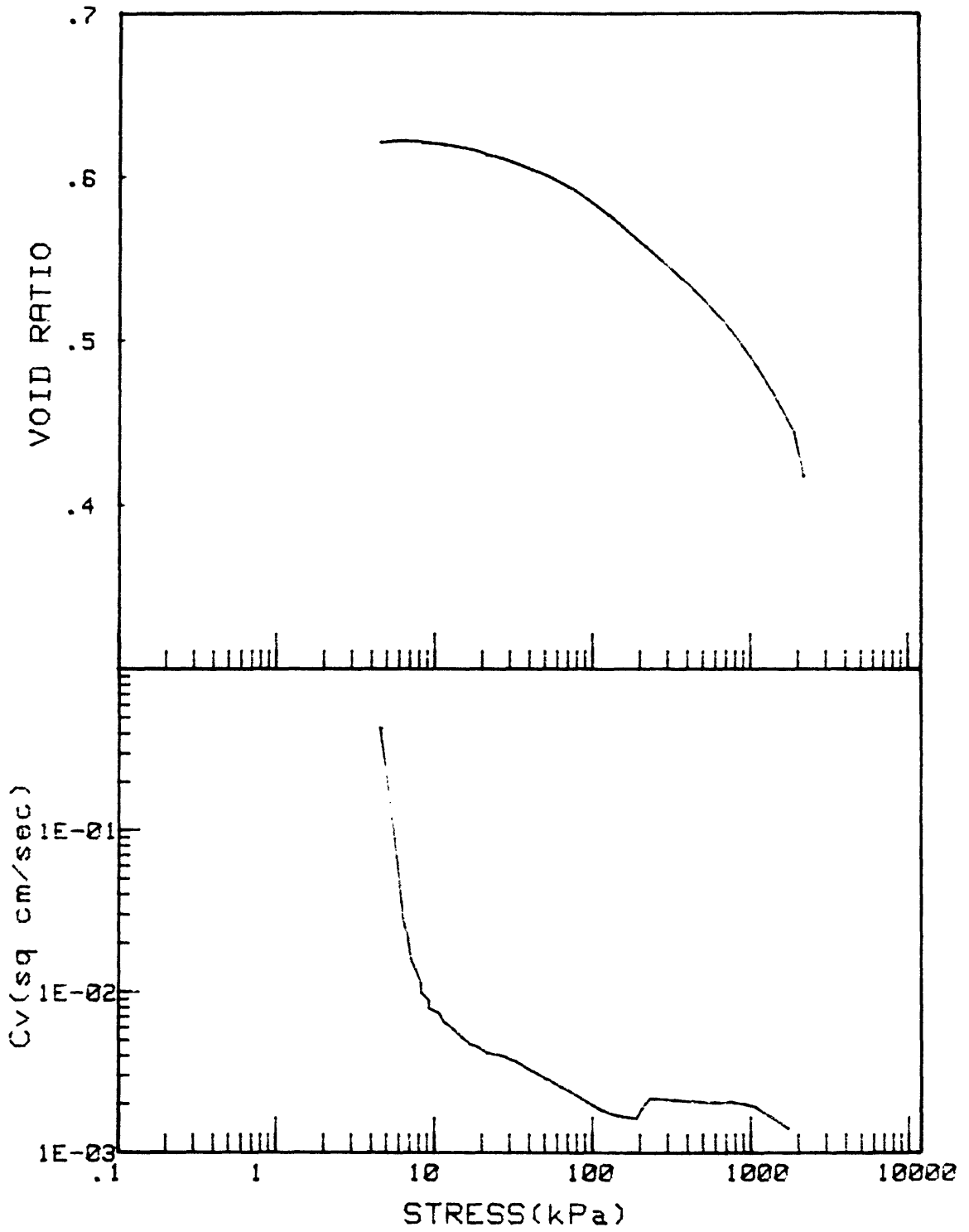
KS1-84-CS	INCREMENT (cm)	SECTION 2
CORE NO.	BORING 3 TEST NO.	CE136



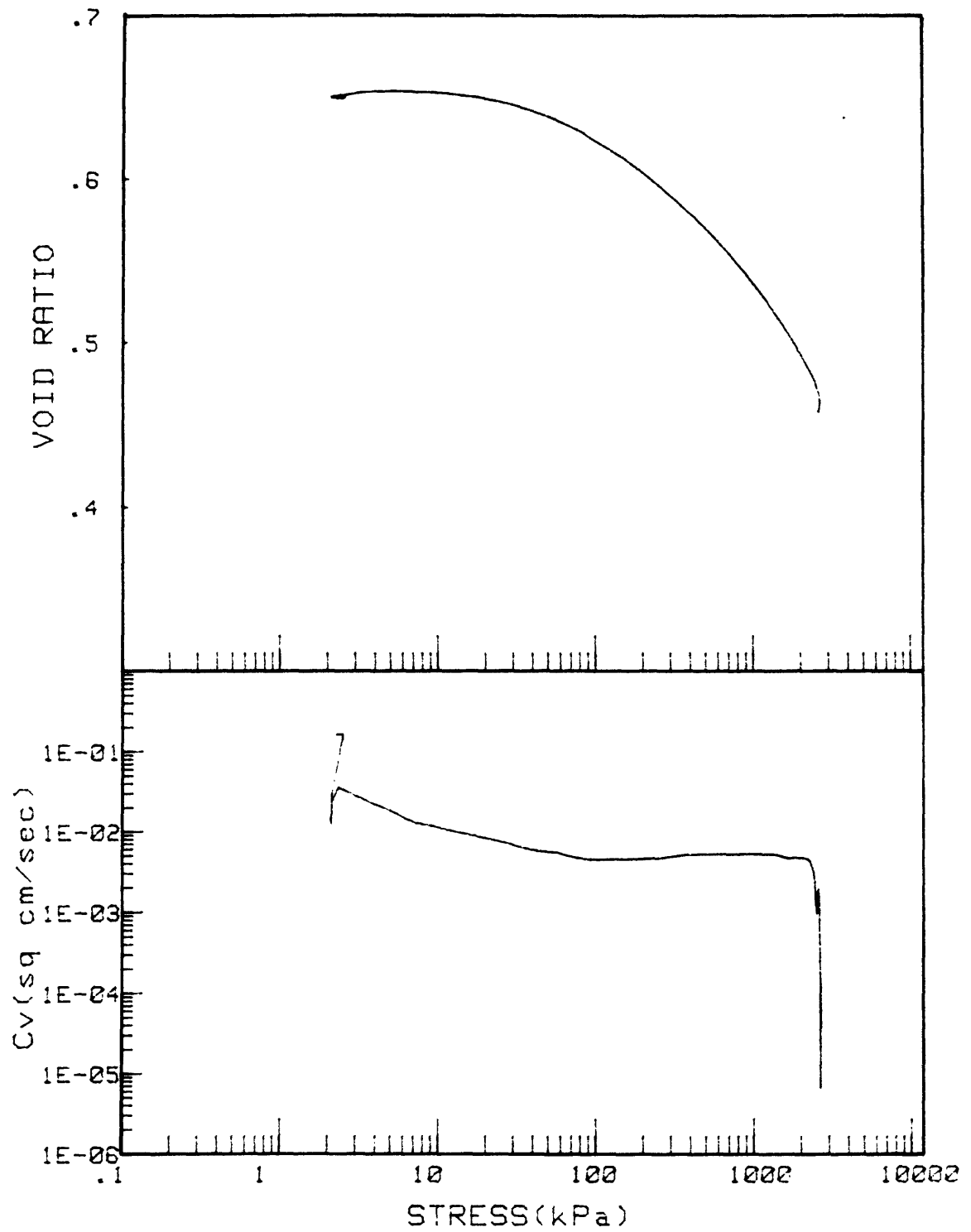
KS1-83-CS	INCREMENT (cm)	SECTION 11
CORE NO.	BORING 3 TEST NO.	CE141



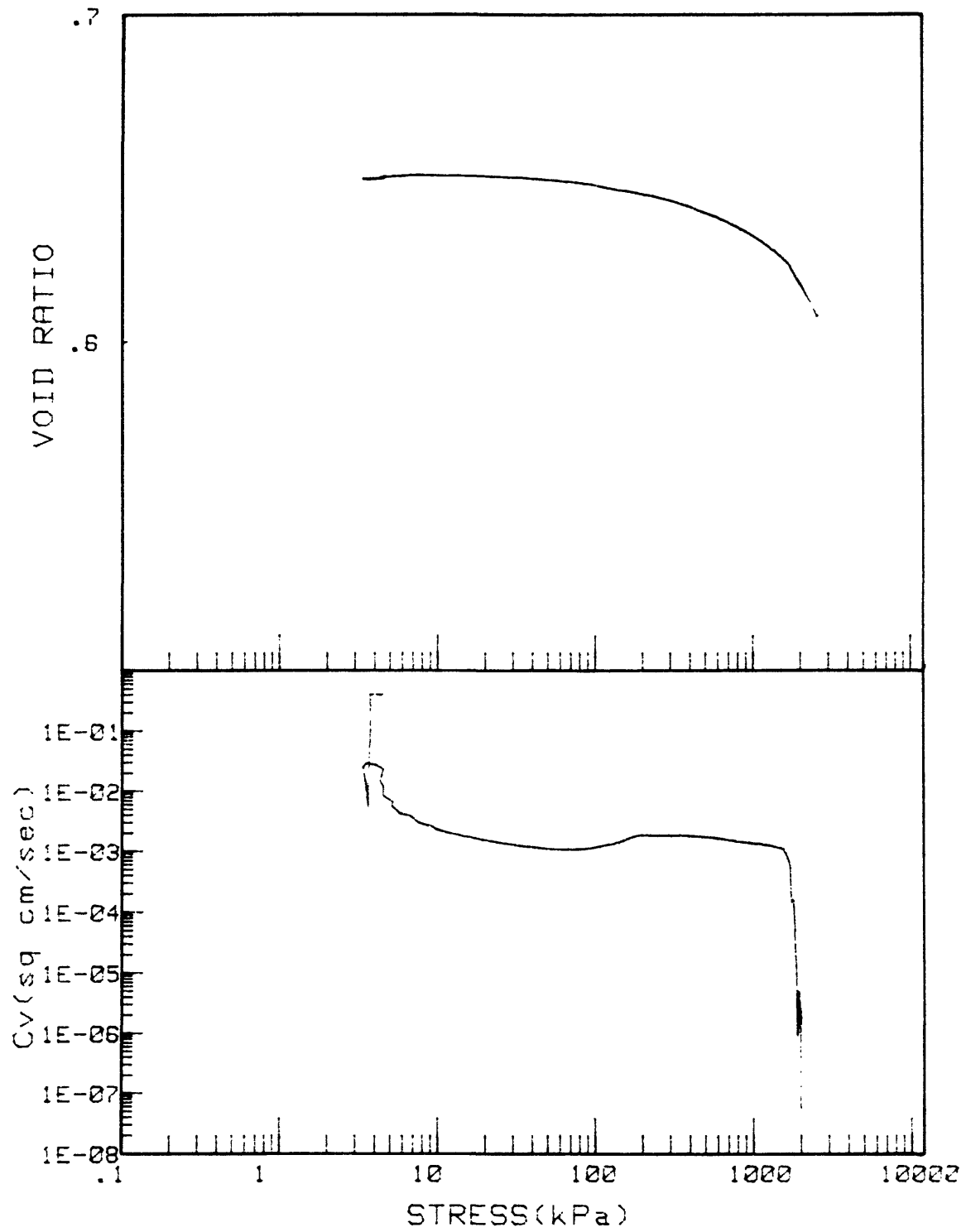
KS1-83-CS	INCREMENT (cm)	SECTION 14
CORE NO.	BORING 3 TEST NO.	CE134



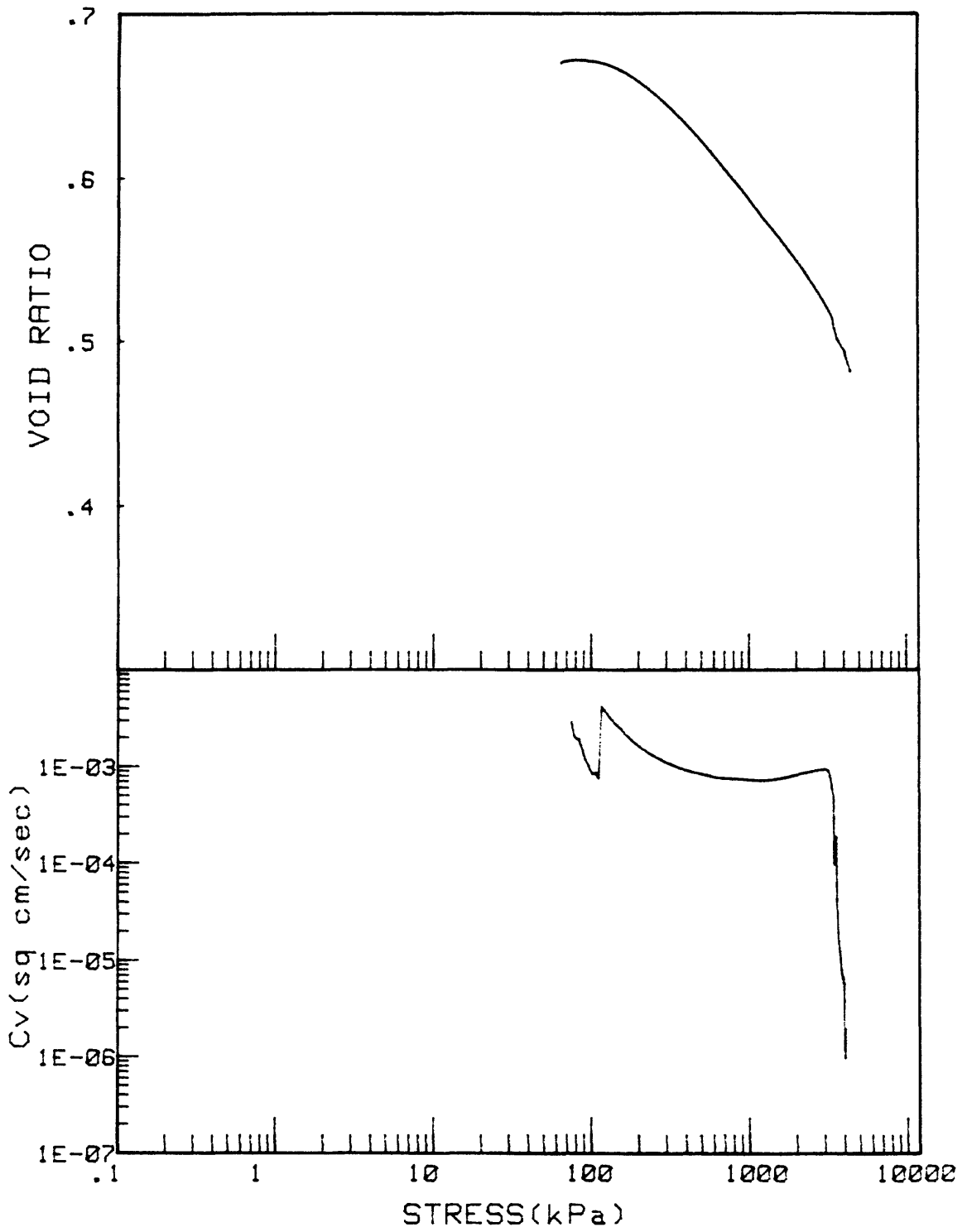
KS1-83-CS	INCREMENT (cm)	SECTION 14
CORE NO.	BORING 3 TEST NO.	CE135



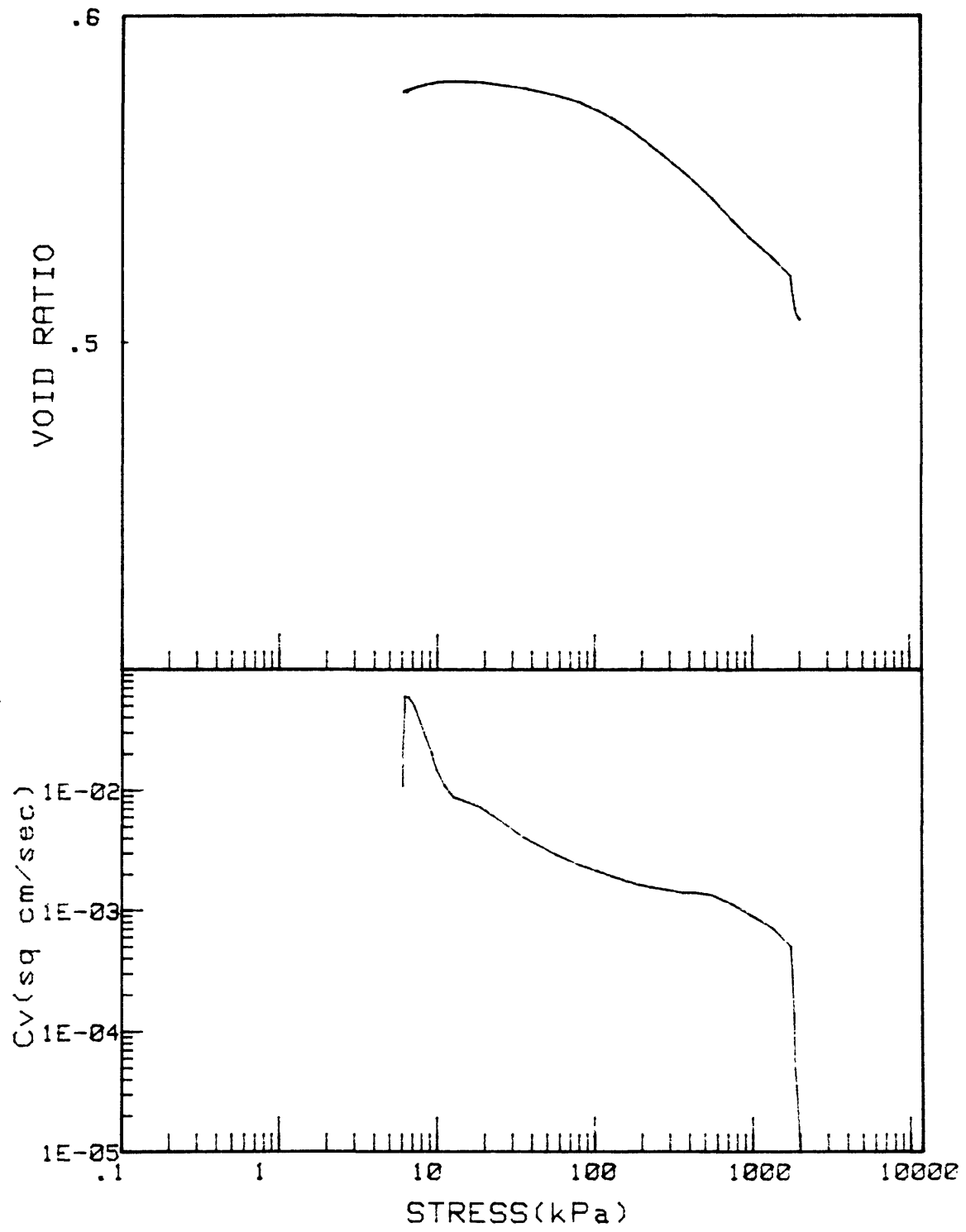
KS1-83-CS		INCREMENT (cm)	19B
CORE NO. B3		TEST NO.	CE167



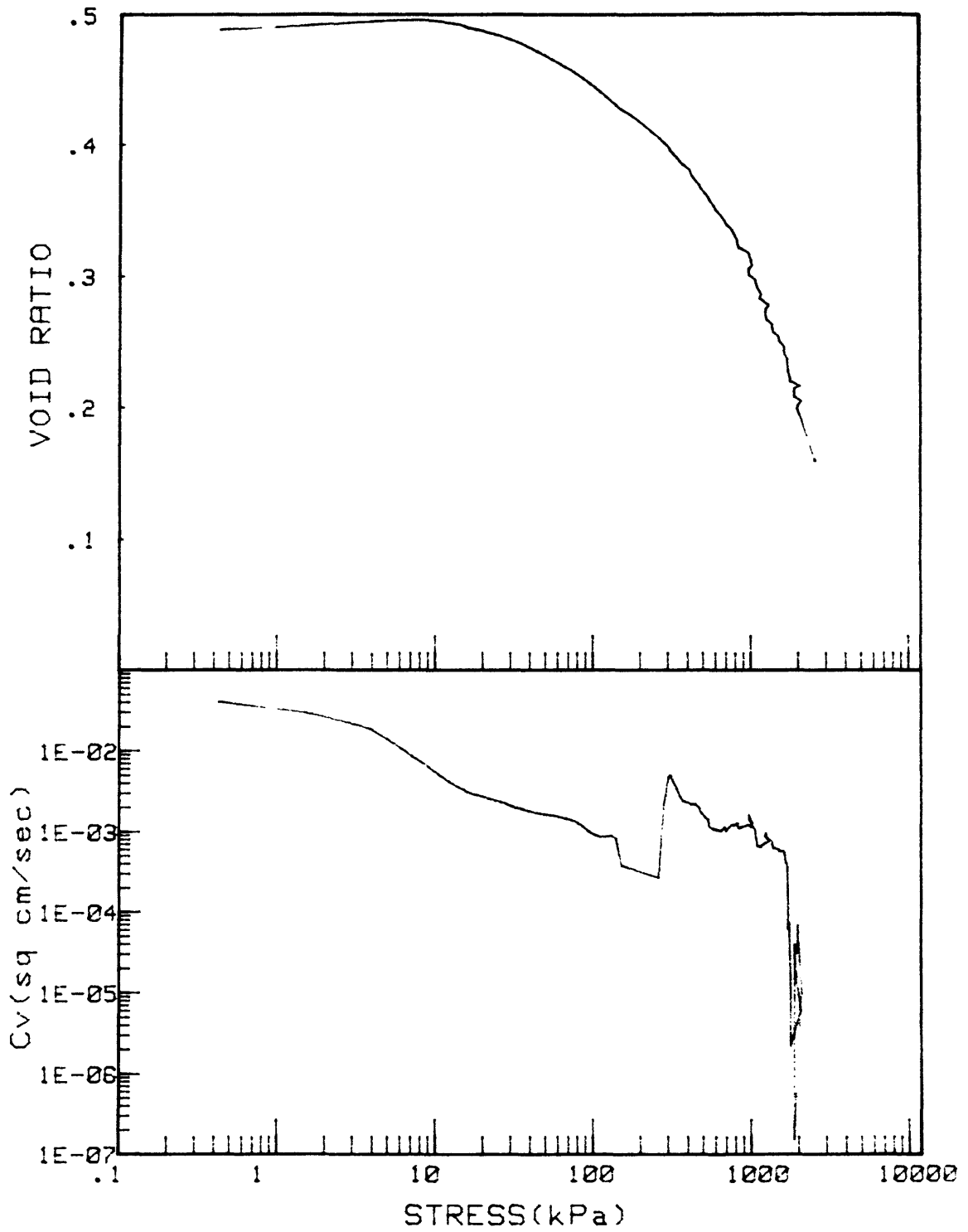
KS1-83-CS	INCREMENT (cm)	28F
CORE NO. B3	TEST NO.	CE168



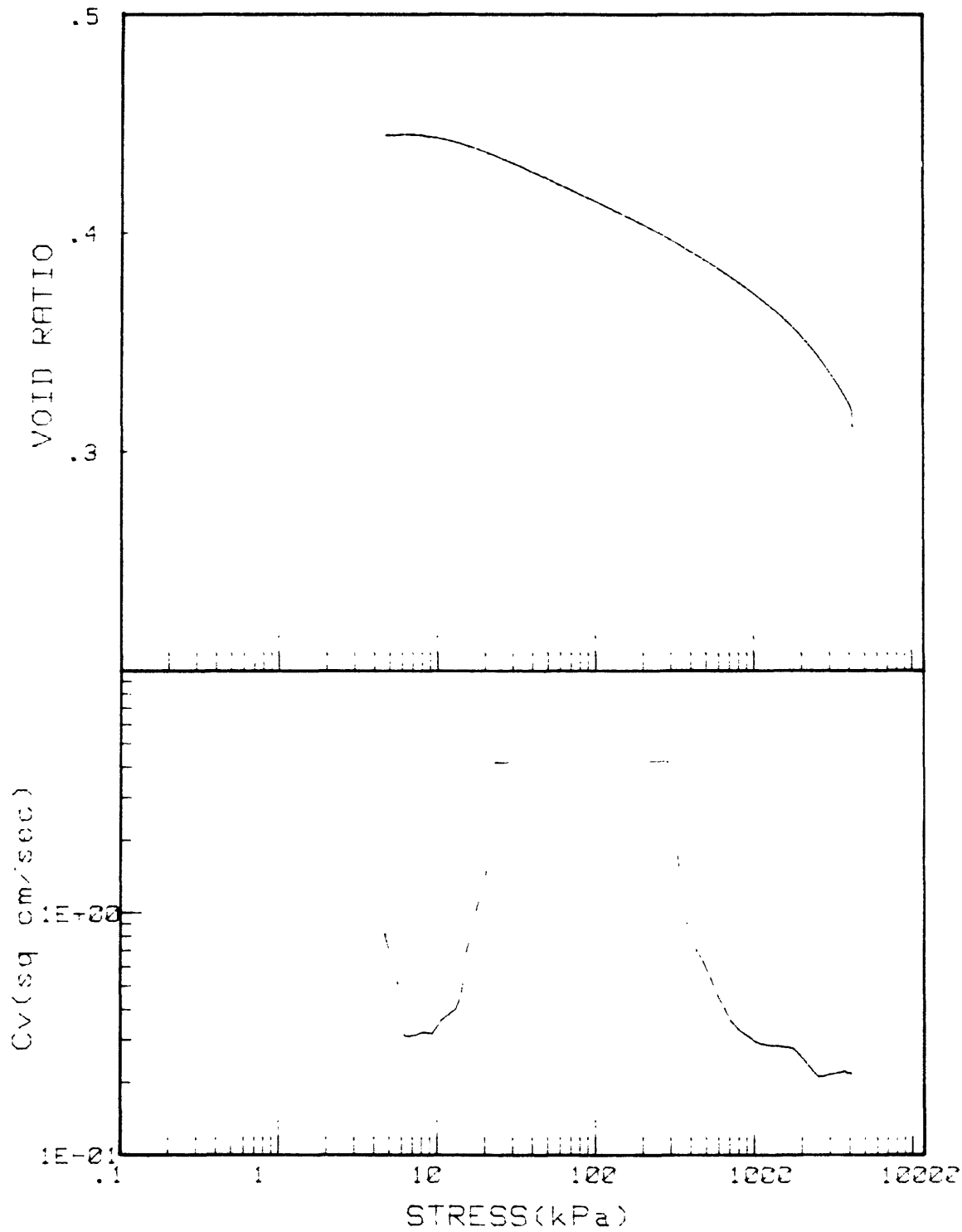
KS1-83-CS	INCREMENT (cm)	S-33I
CORE NO. B-3	TEST NO.	CE150



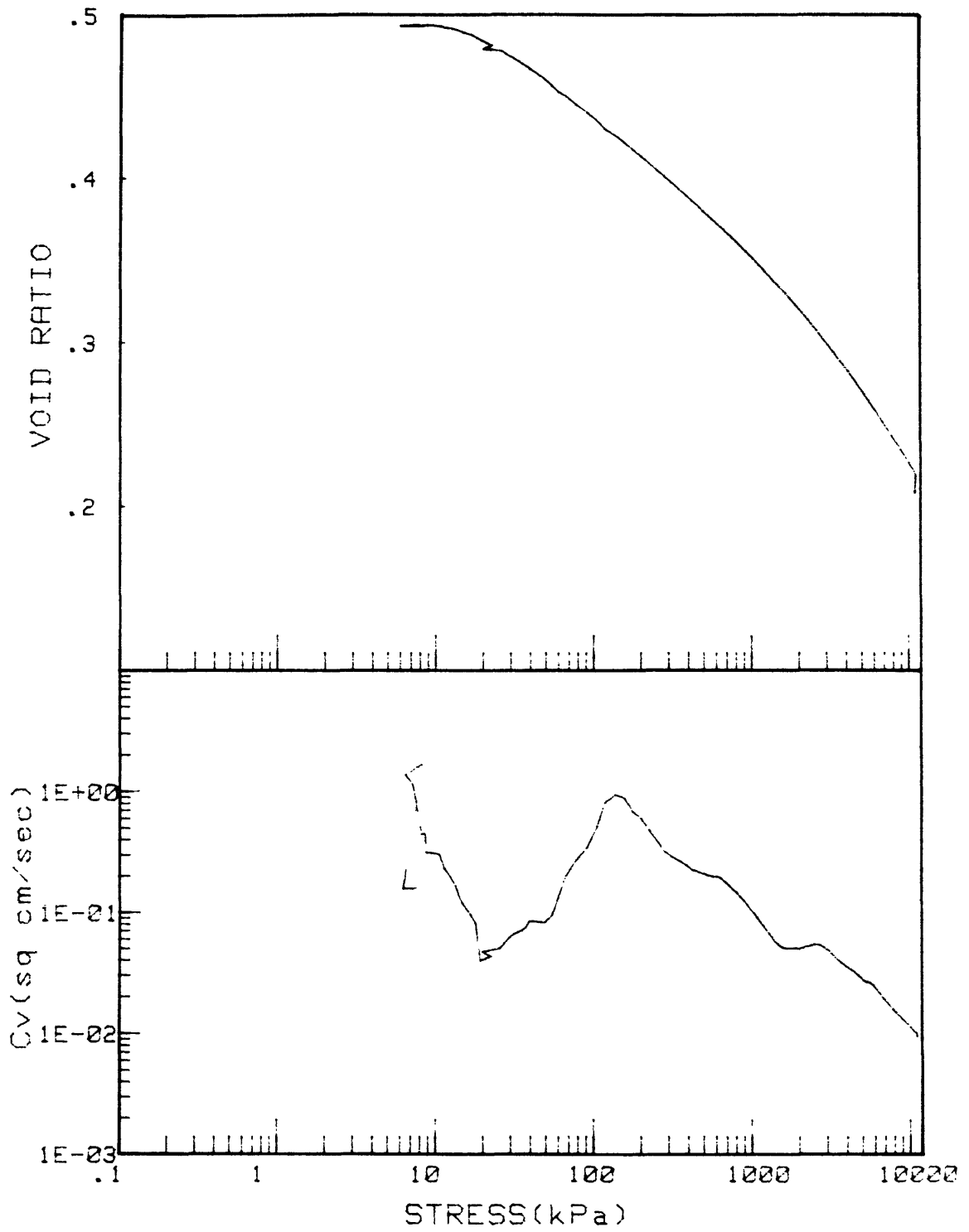
KS1-83-CS		INCREMENT (cm)	S-38H
CORE NO. B-3		TEST NO.	CE172



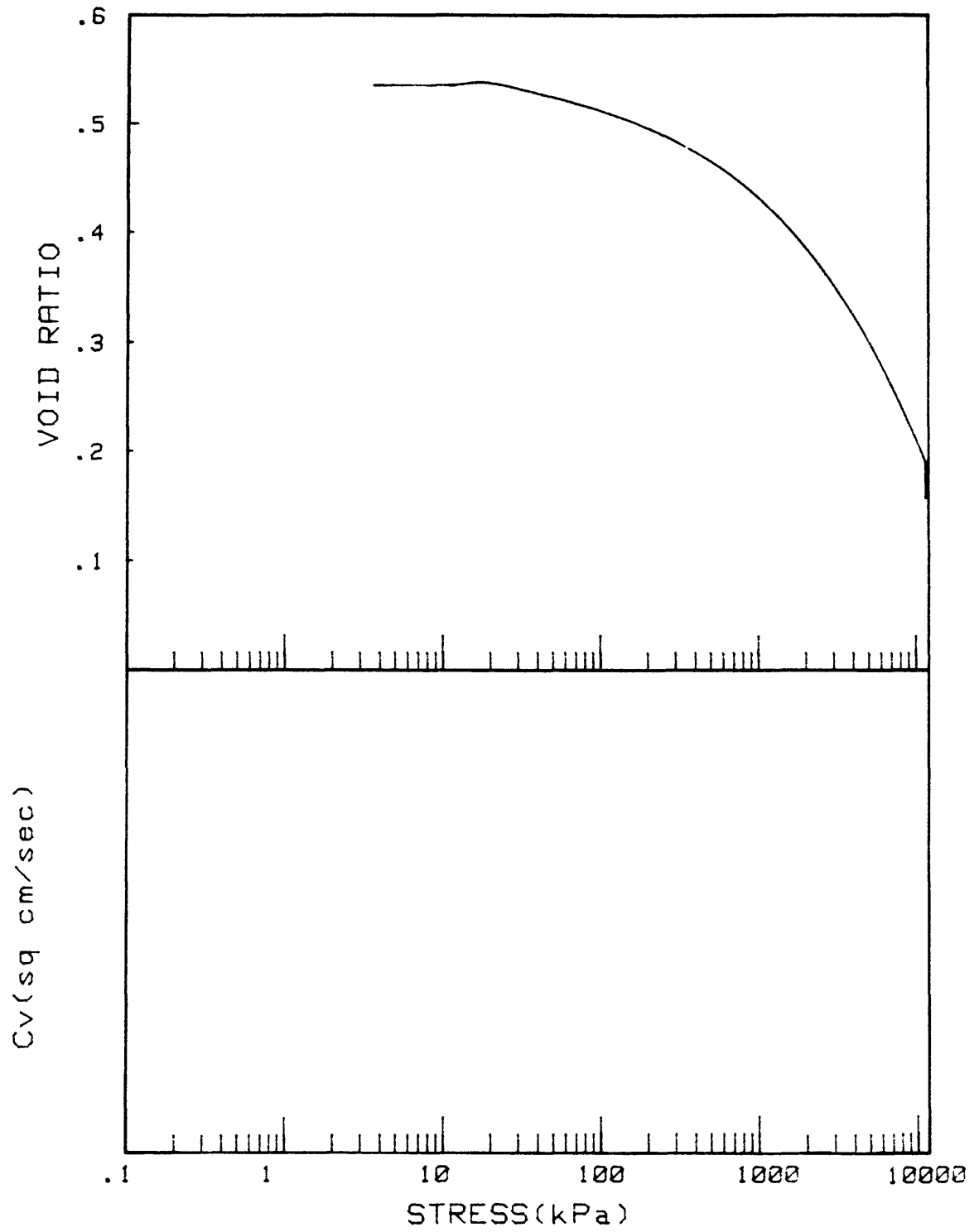
KSI-83-CS		INCREMENT (cm)	S-43E
CORE NO. B-3		TEST NO.	CE173



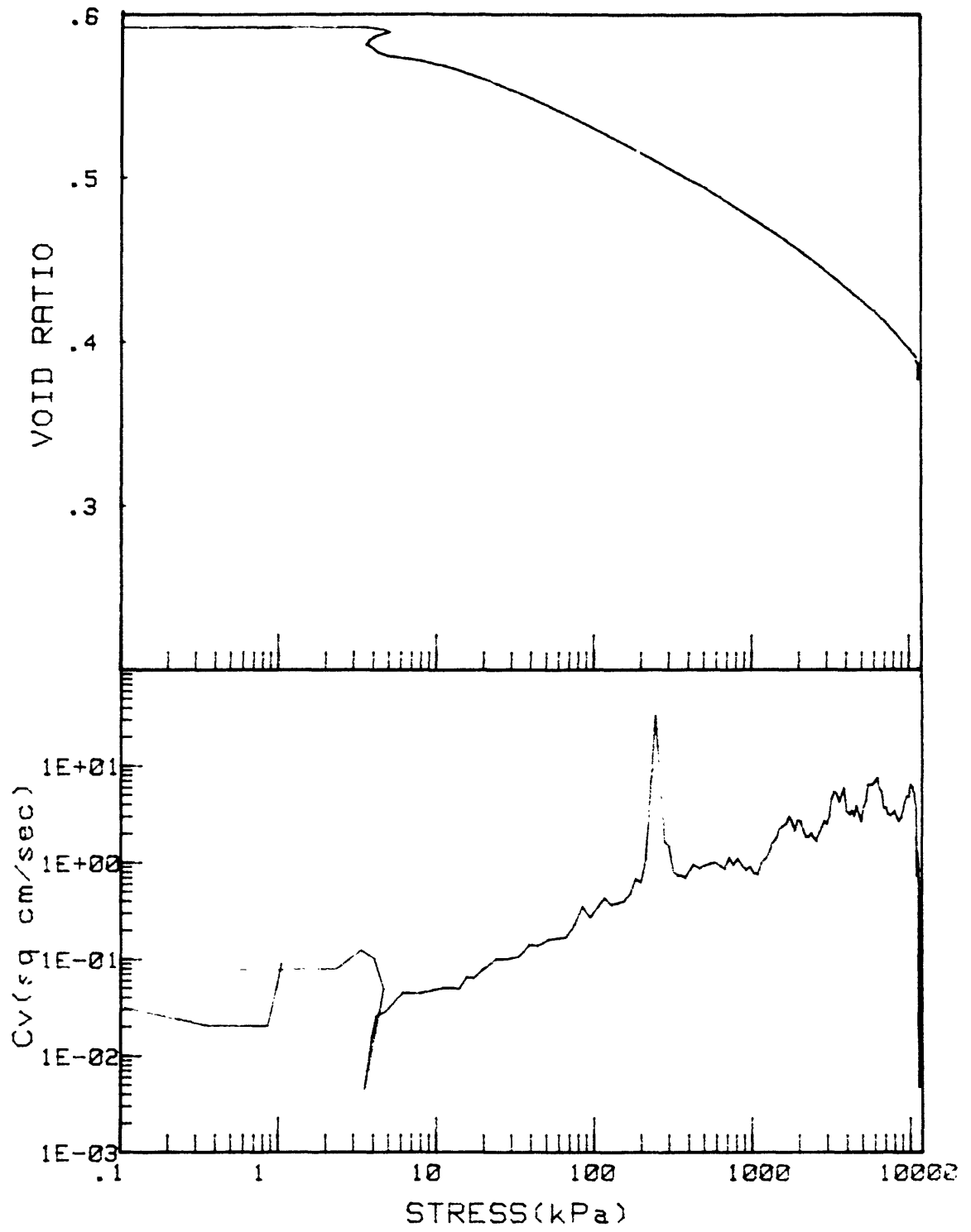
KS1-83-CS	INCREMENT (cm)	SECTION 1
CORE NO.	BORING 7 TEST NO.	CE146



KS1-83-CS	INCREMENT (cm)	SECTION 21
CORE NO.	BORING 7 TEST NO.	CE147



KS1-83-CS	INCREMENT (cm)	S-24
CORE NO. B-7	TEST NO.	CE148

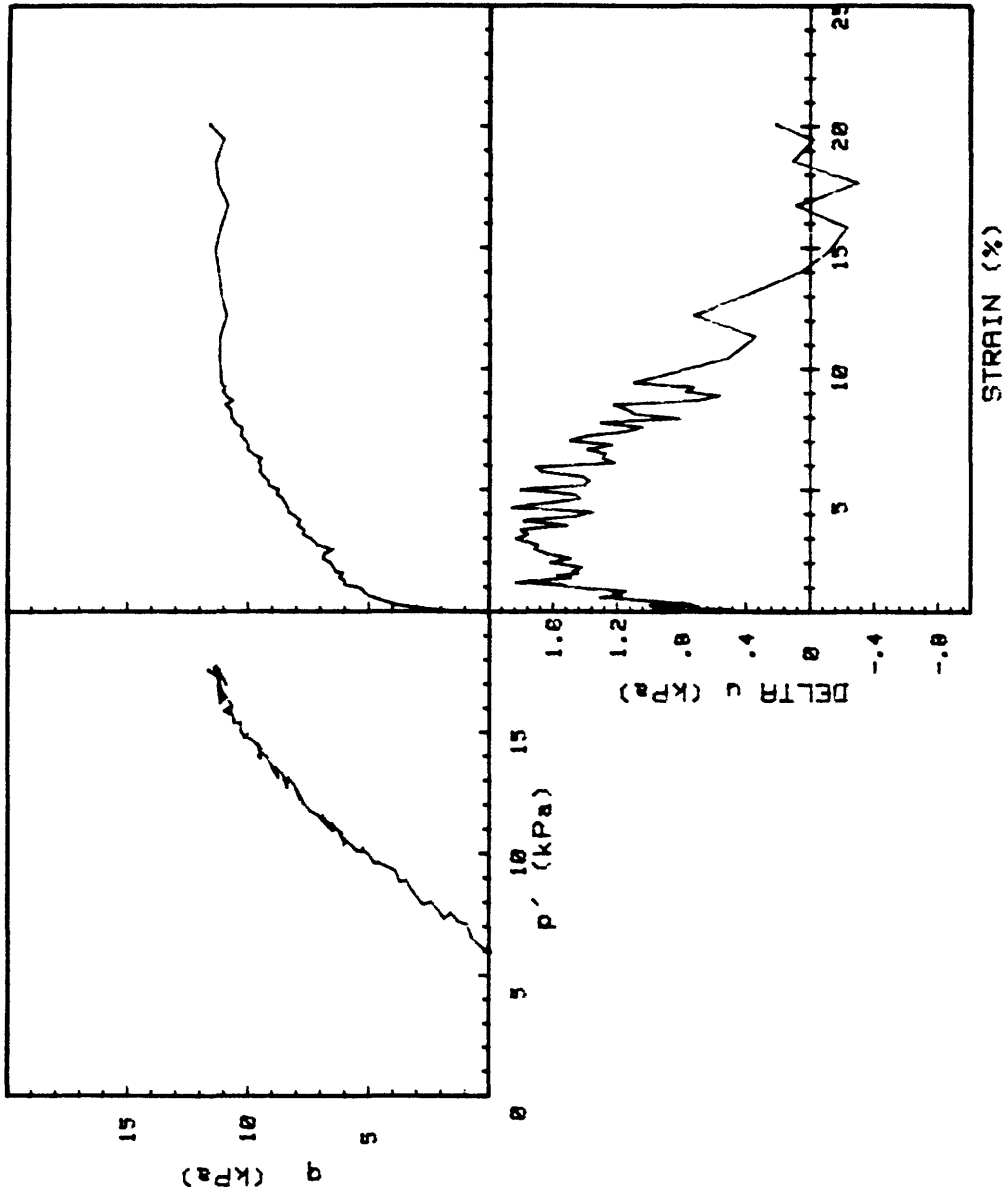


KS1-83-CS		INCREMENT (cm)	S-1
CORE NO. B-8		TEST NO.	CE174

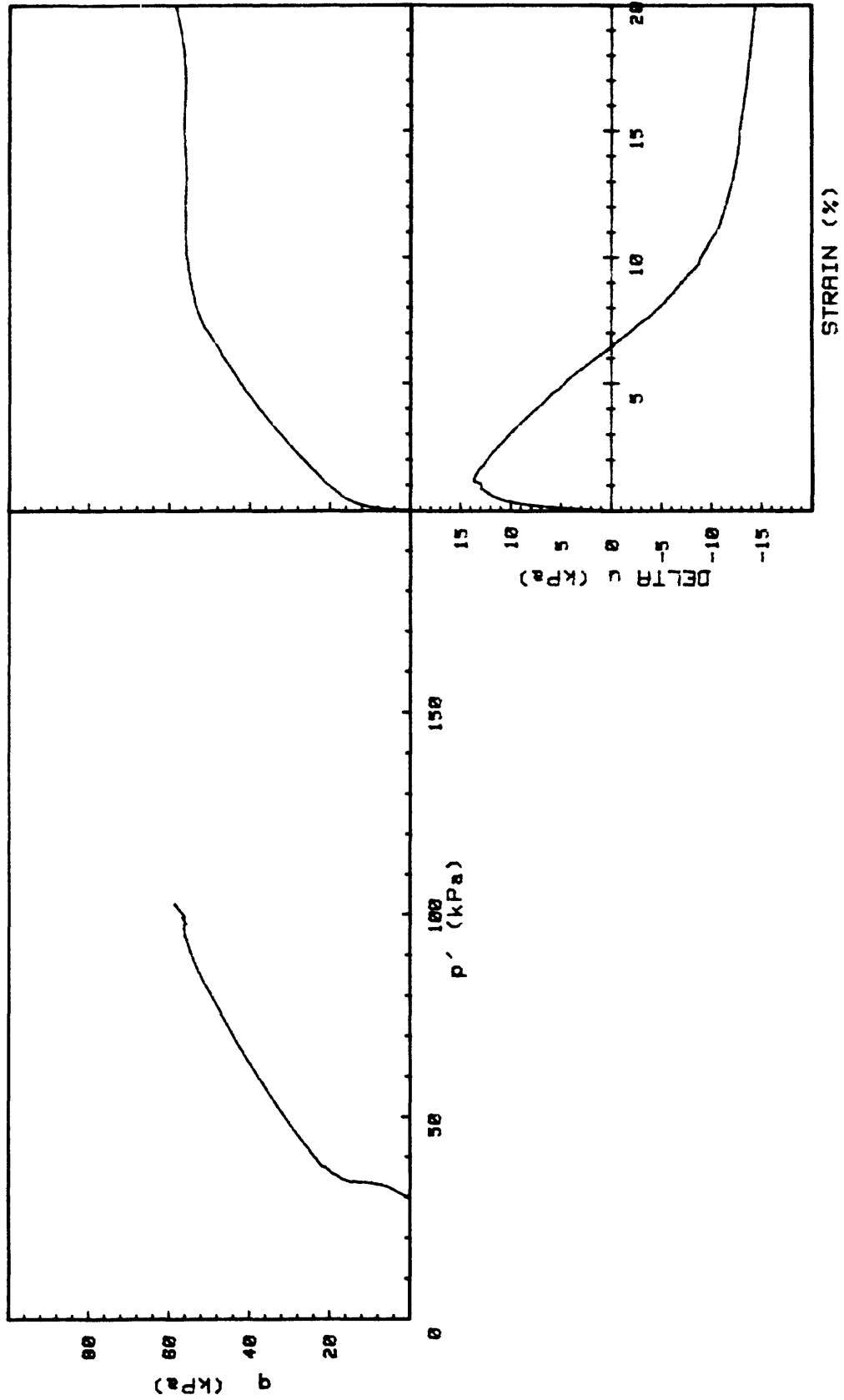
APPENDIX B

TRIAXIAL AND UNCONFINED COMPRESSION

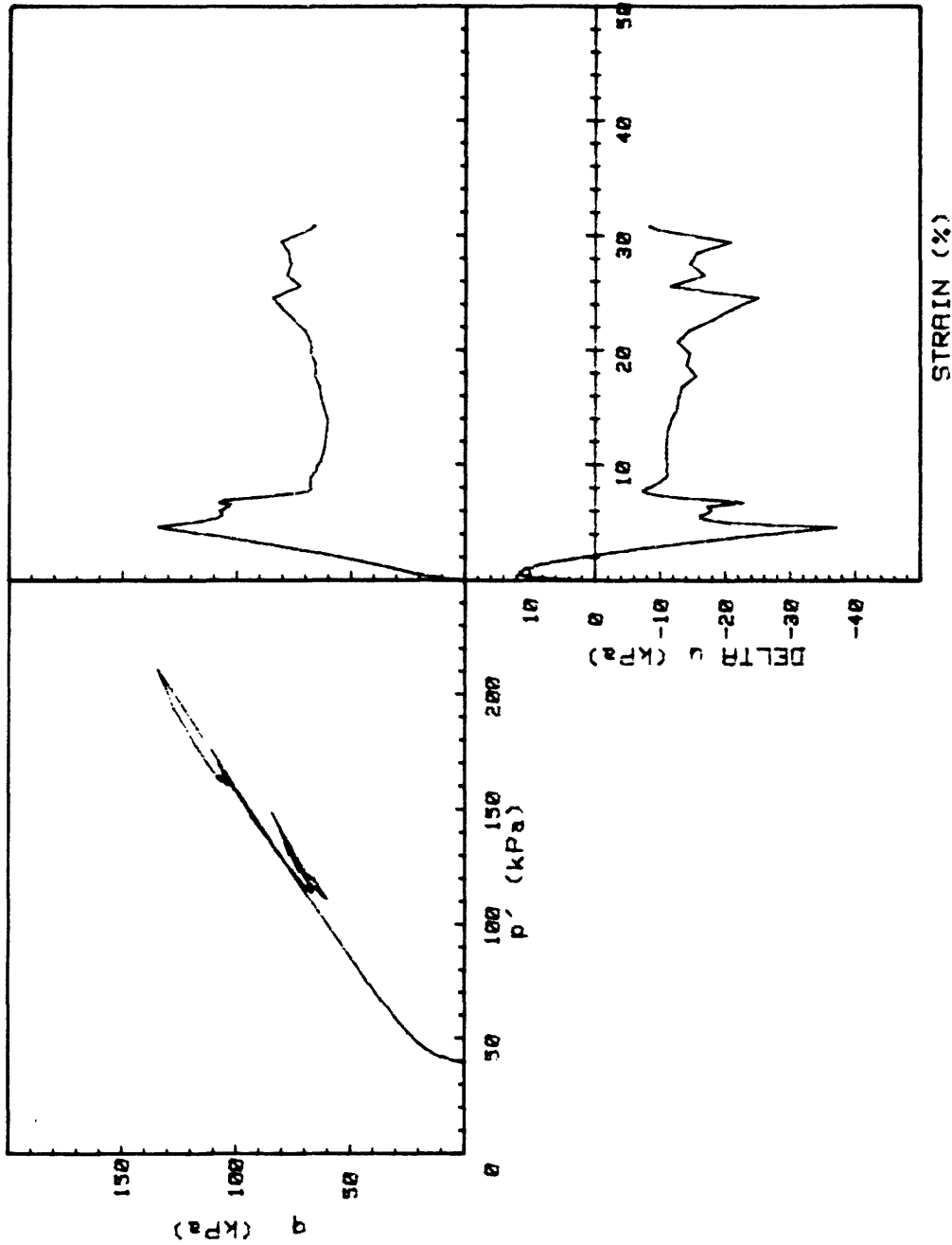
TEST RESULTS



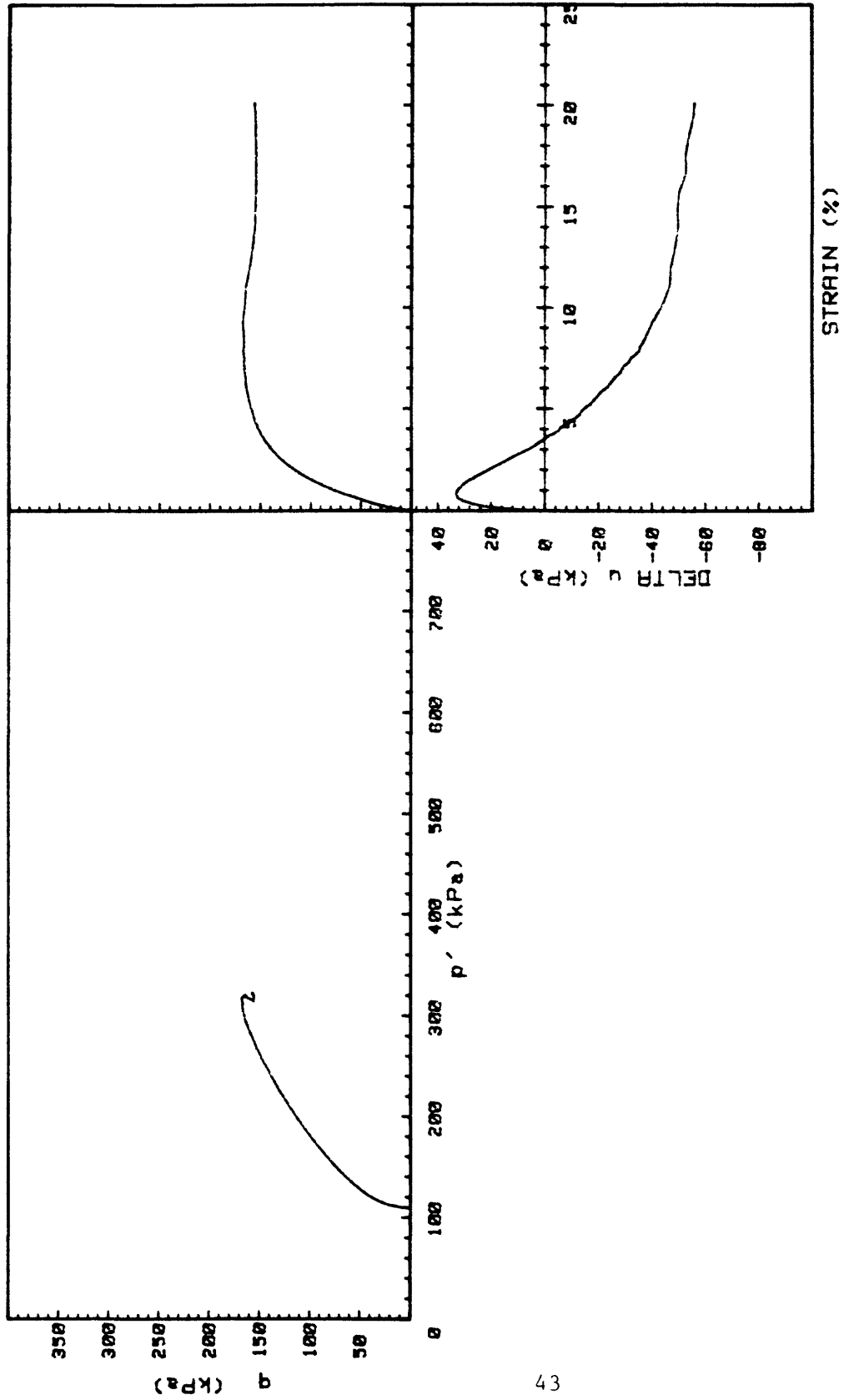
KSI-83-CS	INCREMENT (cm)	S-2
CORE NO. B-2	TEST NO.	TE258
SIG1c' (kPa)	6.2	
SIG3c' (kPa)	6.2	
INDUCED OCR	1.0	



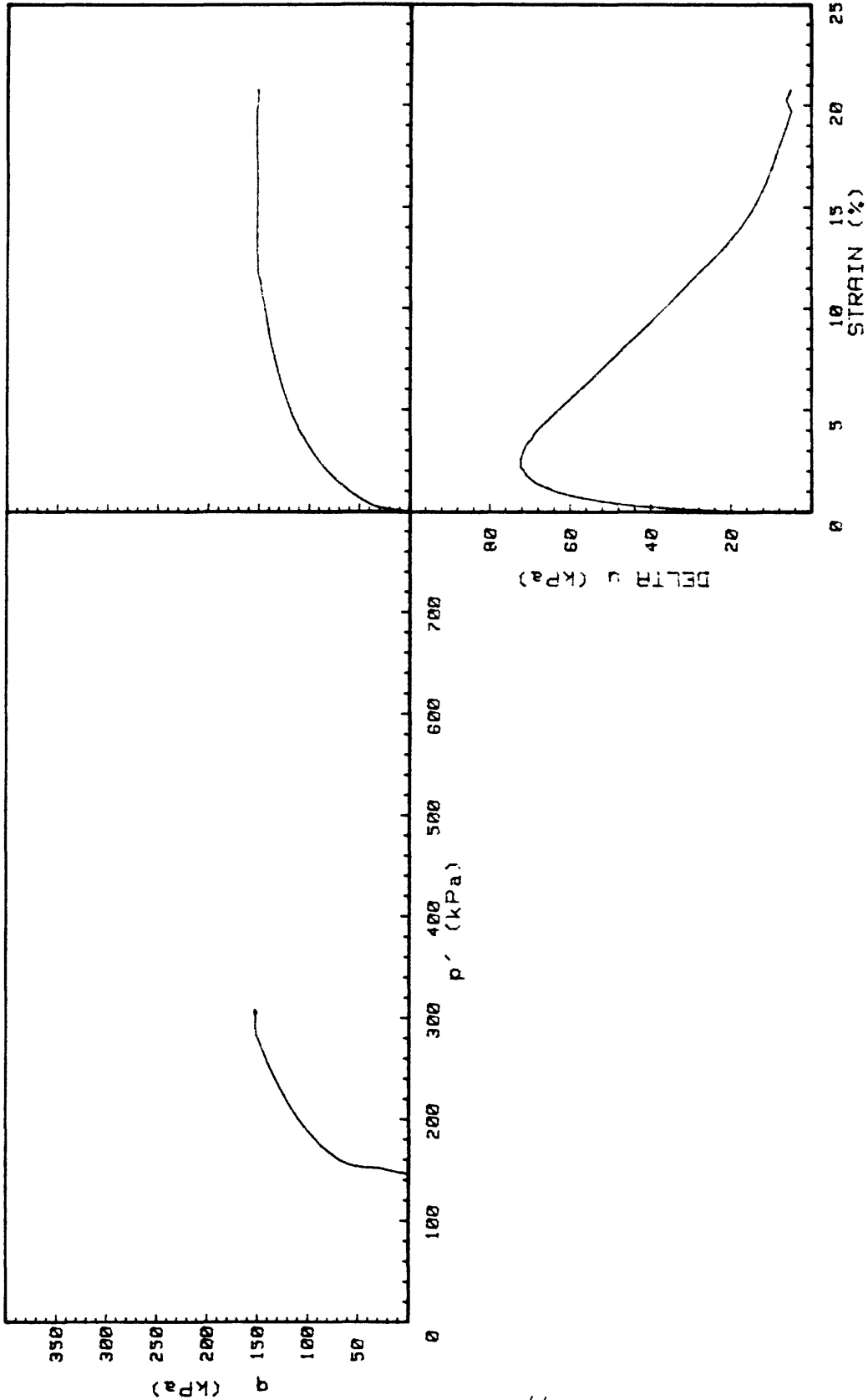
K51-83-CS	INCREMENT (cm)	S-6
CORE NO. B-2	TEST NO.	TE257
SIG1c' (kPa) 29.7		
SIG3c' (kPa) 29.7		
INDUCED OCR 1.0		



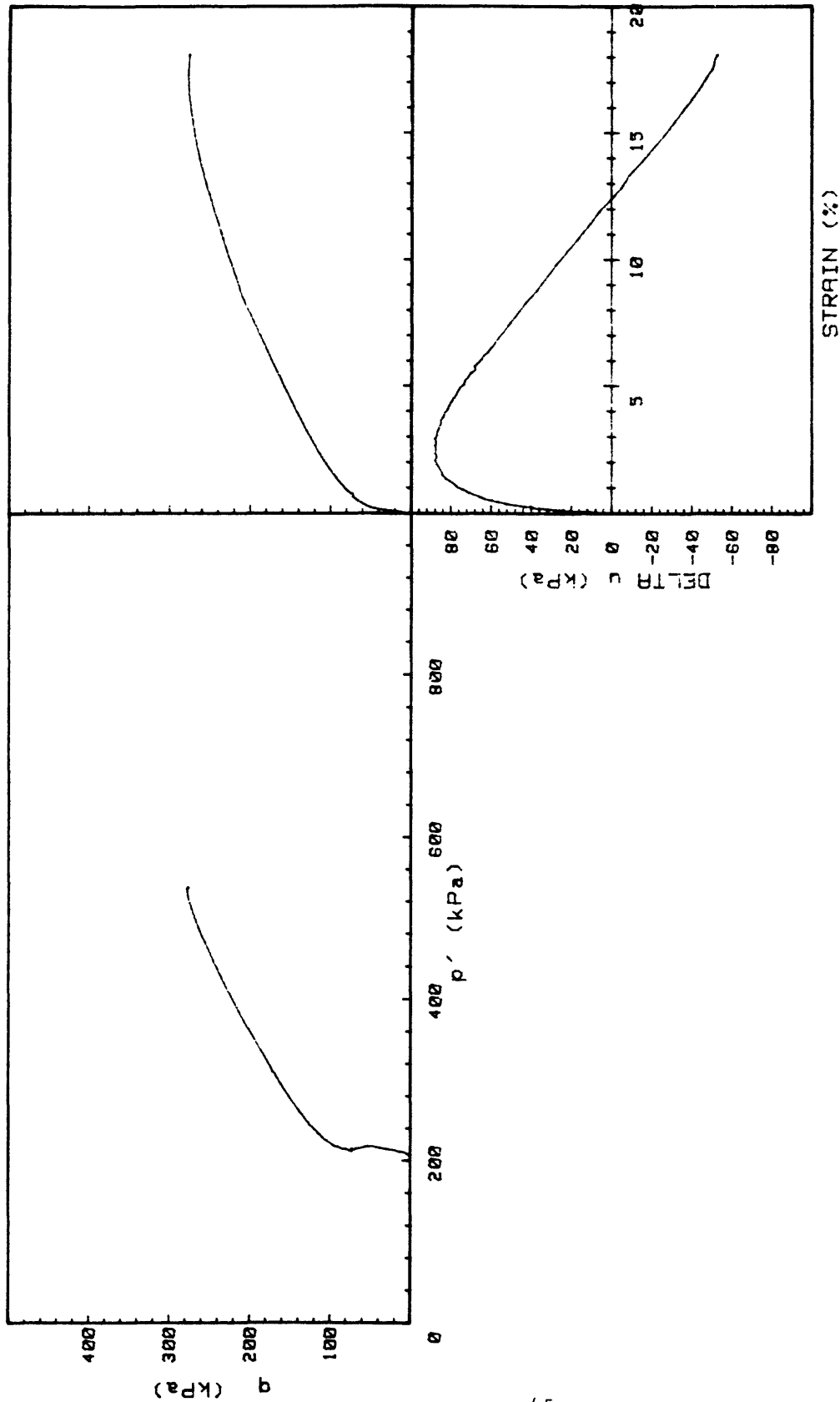
KSI-83-CS	INCREMENT (cm)	S-2
CORE NO. B-3	TEST NO.	TE259
SIG <sub>1c</sub> ' (kPa)		39.3
SIG <sub>3c</sub> ' (kPa)		39.3
INDUCED OCR		1.0



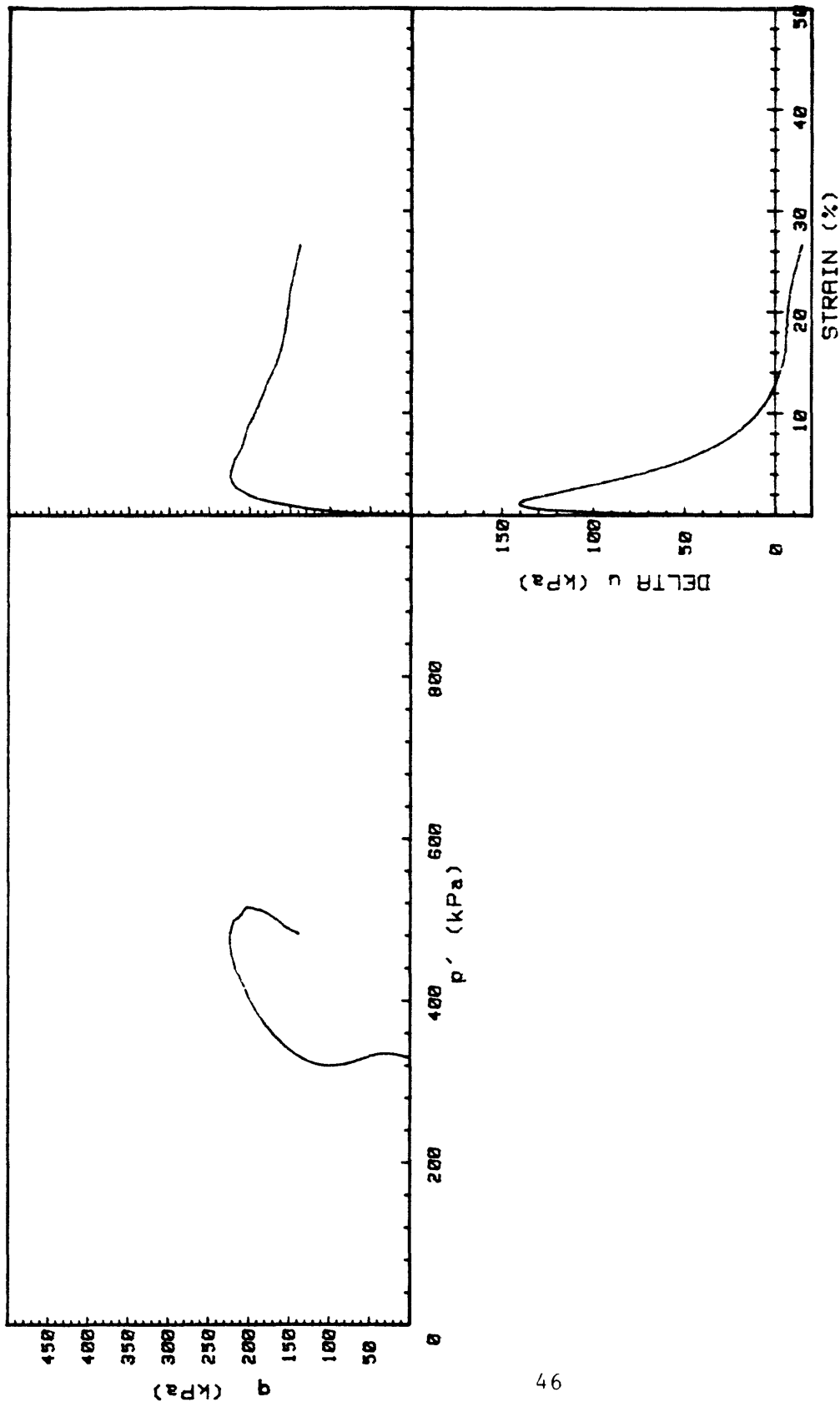
KSI-03-CS	INCREMENT (cm)	S-14
CORE NO. B-3	TEST NO.	TE260
SIG1c' (kPa)	109.7	
SIG3c' (kPa)	109.7	
INDUCED OCR	1.0	



K51-83-CS	INCREMENT (cm)	19B
CORE NO. B-3	TEST NO.	TE265
SIG1c' (kPa)	160.4	
SIG3c' (kPa)	160.4	
INDUCED OCR	1.0	

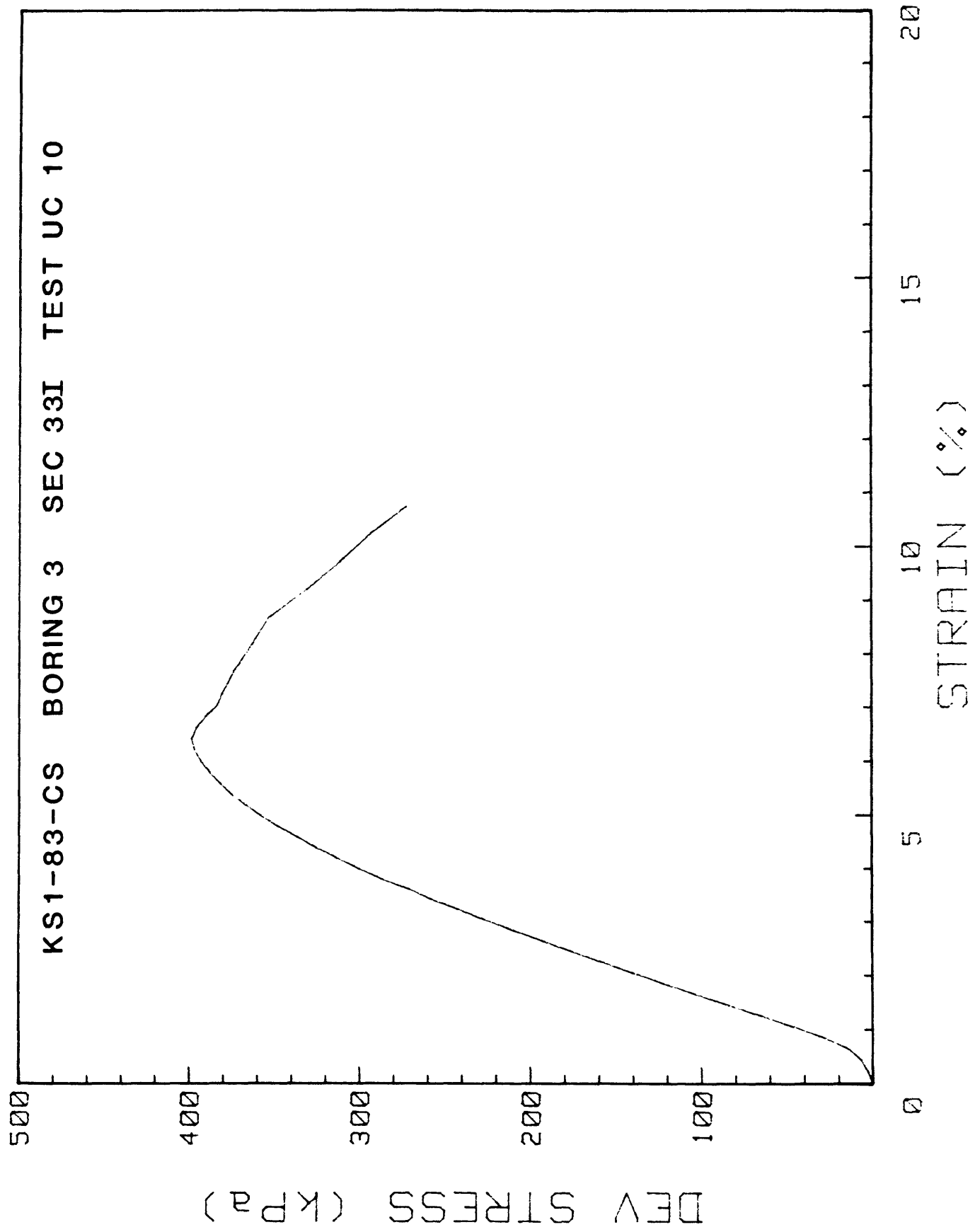


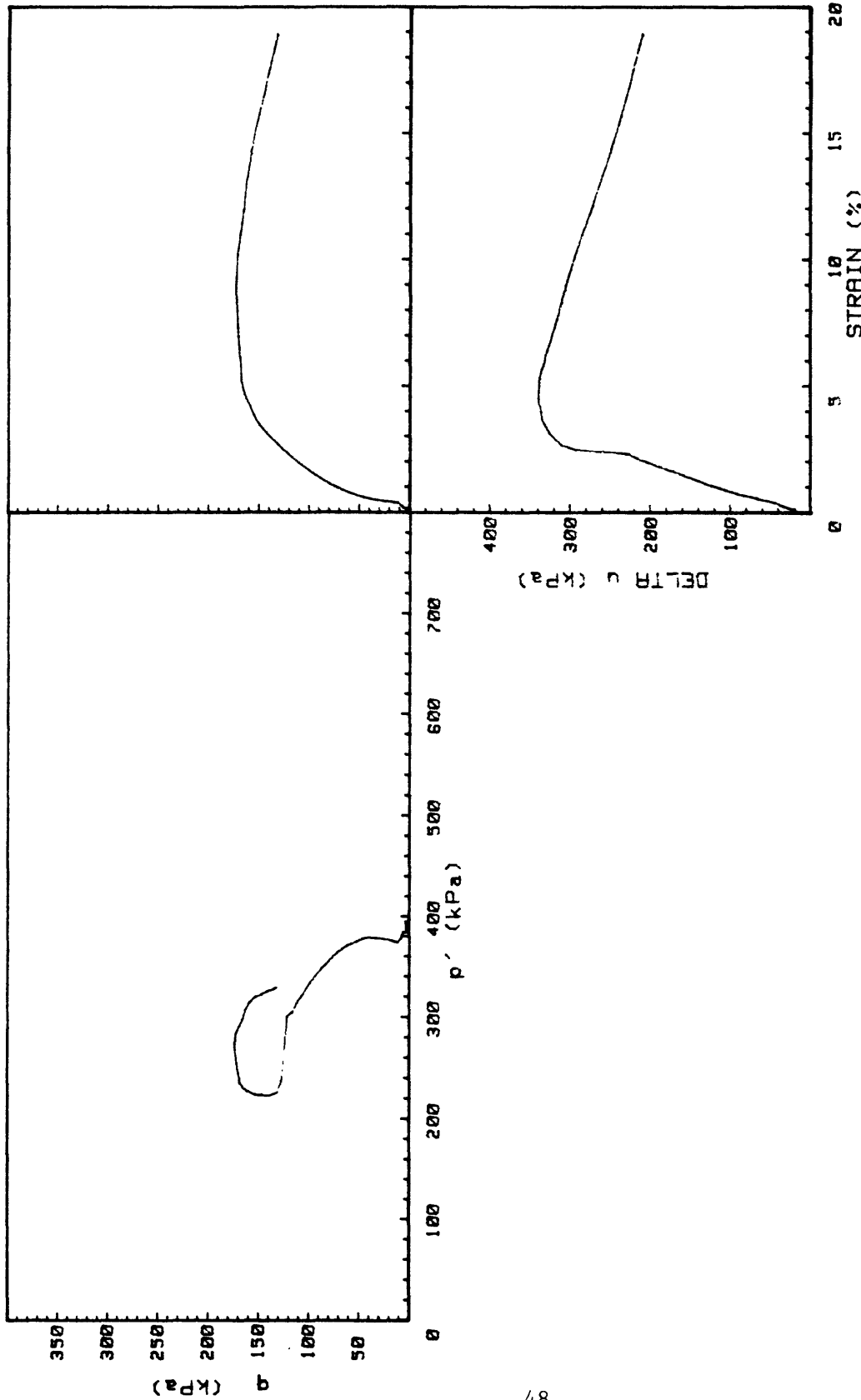
KSI-83-CS	INCREMENT (cm)	28F
CORE NO. B-3	TEST NO.	TE266
SIG1c' (kPa)	208.8	
SIG3c' (kPa)	208.8	
INDUCED OCR	1.0	



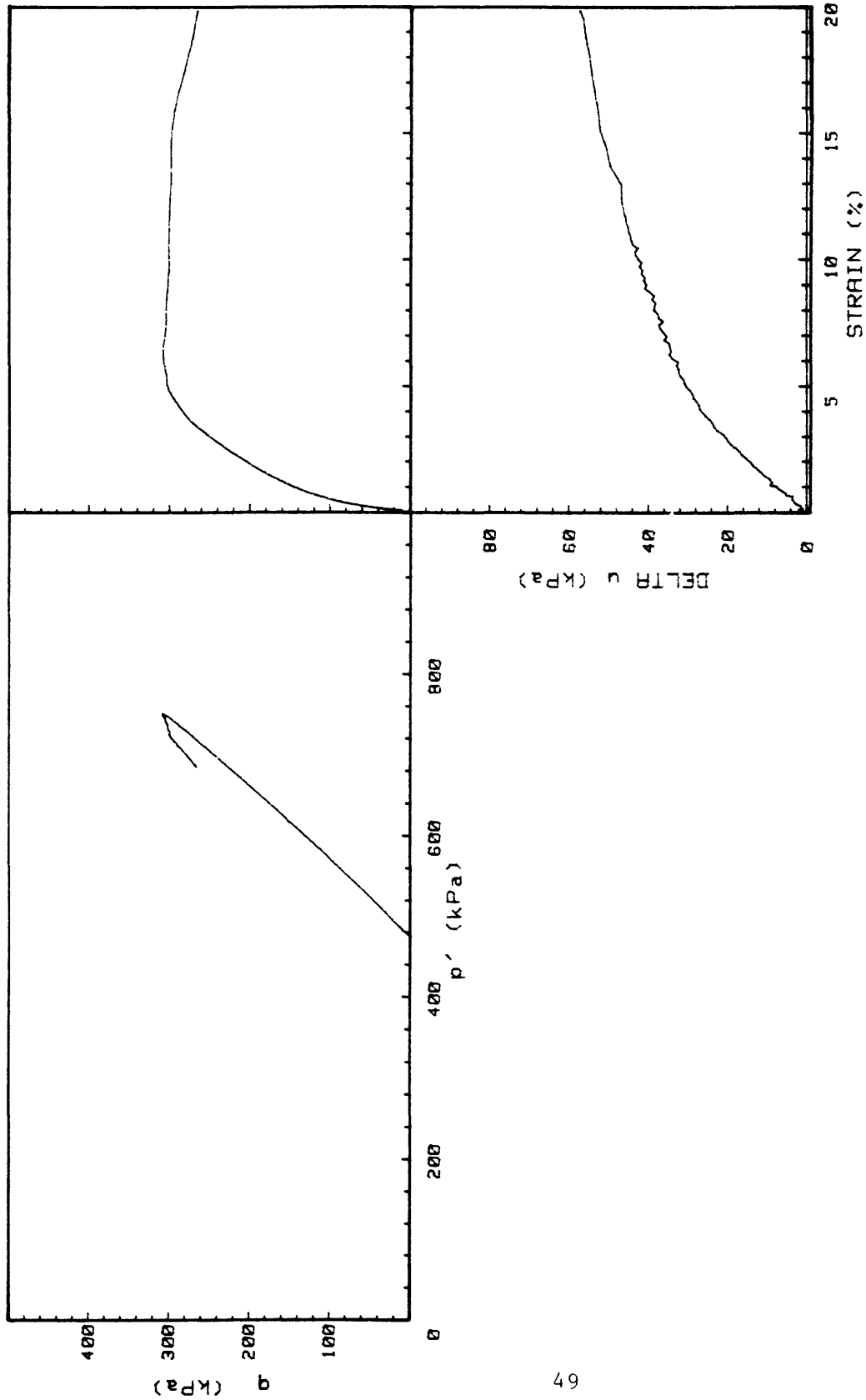
KSI-83-CS	INCREMENT (cm)	S33-I
CORE NO. B-3	TEST NO.	TE264
SIG1c' (kPa)	329.8	
SIG3c' (kPa)	329.8	
INDUCED OCR	1	

KS1-83-CS BORING 3 SEC 33I TEST UC 10

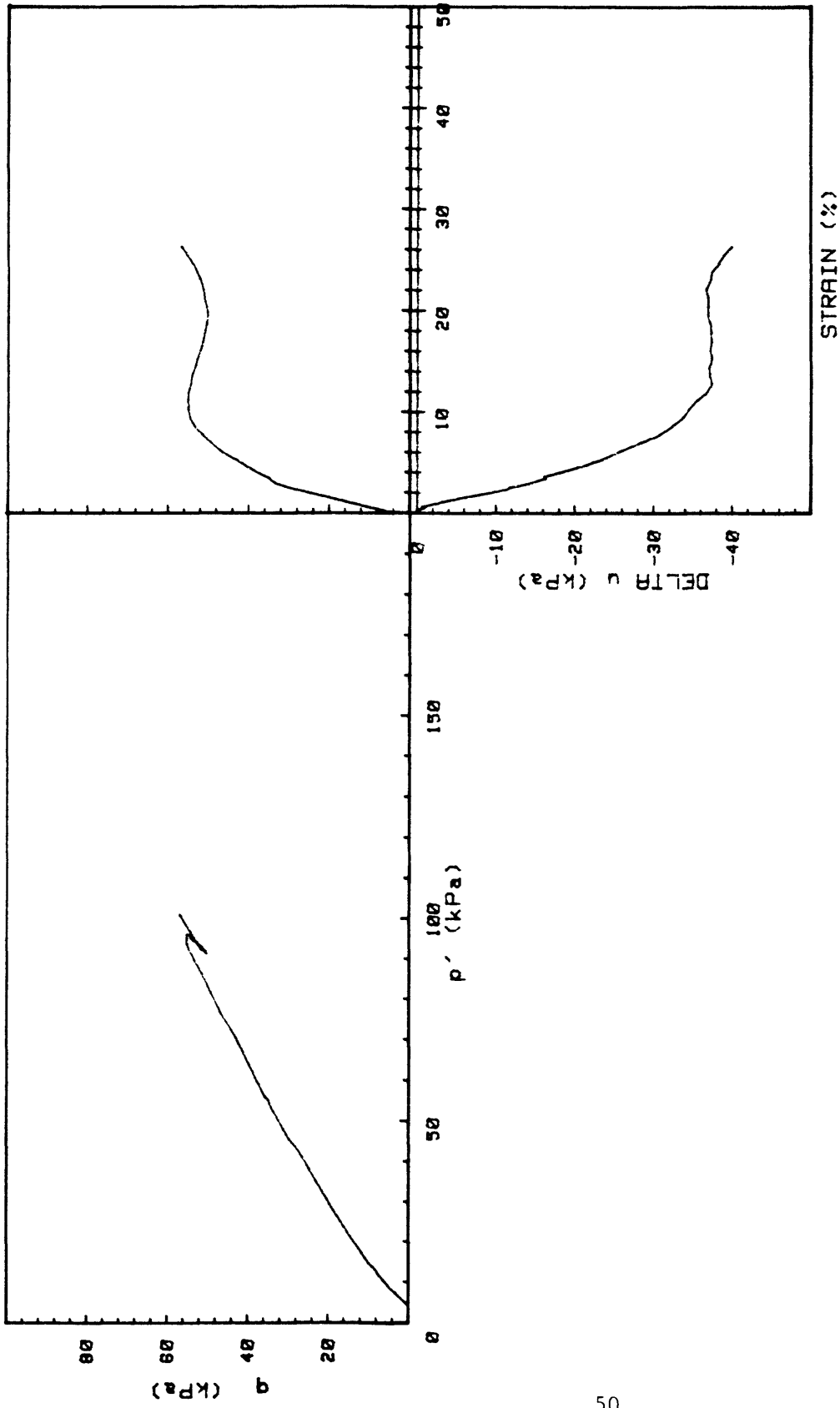




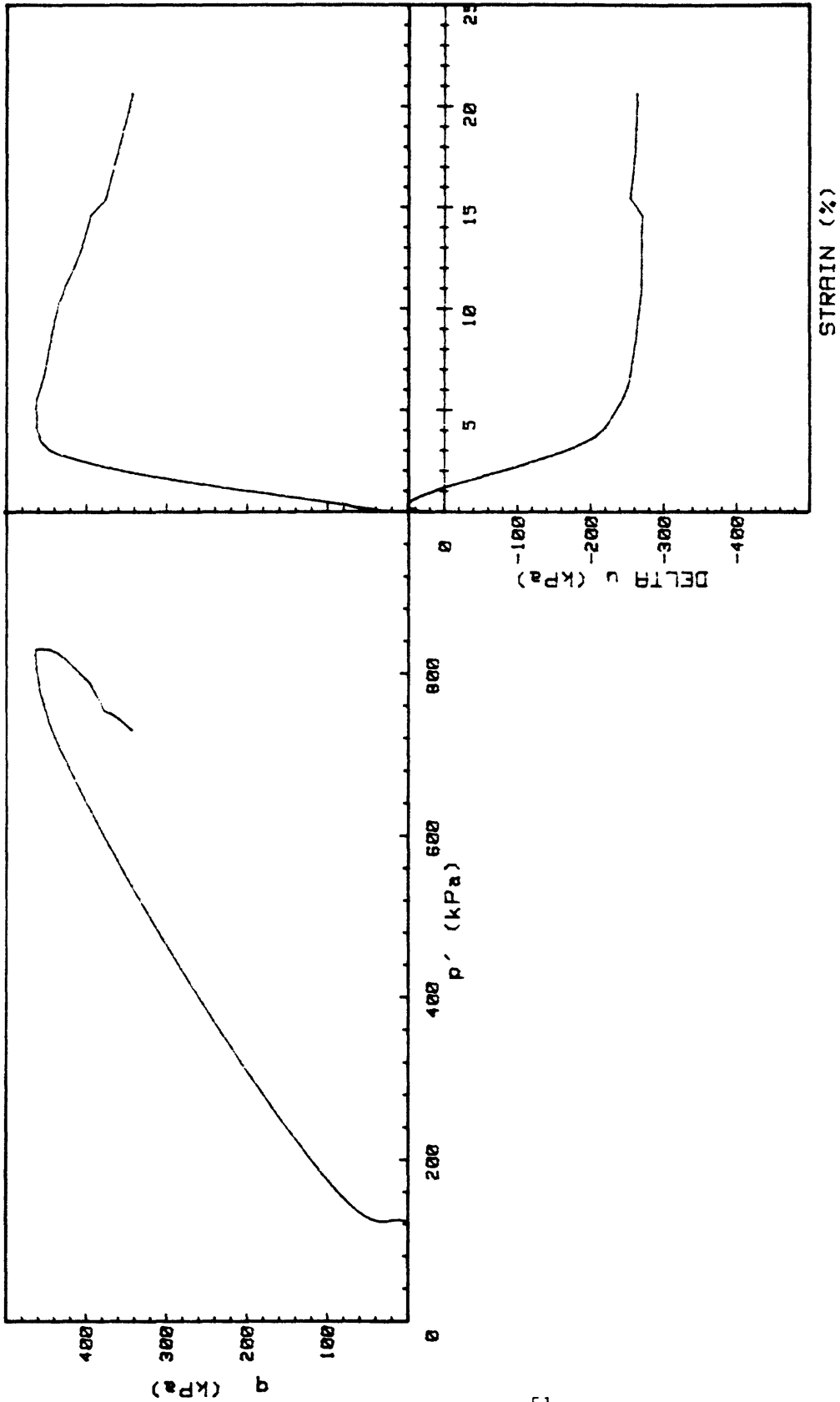
KSI-83-CS	INCREMENT (cm)	S-38H
CORE NO. B-3	TEST NO.	TE270
SIG1c' (kPa)	405.9	
SIG3c' (kPa)	405.9	
INDUCED OCR	1.0	



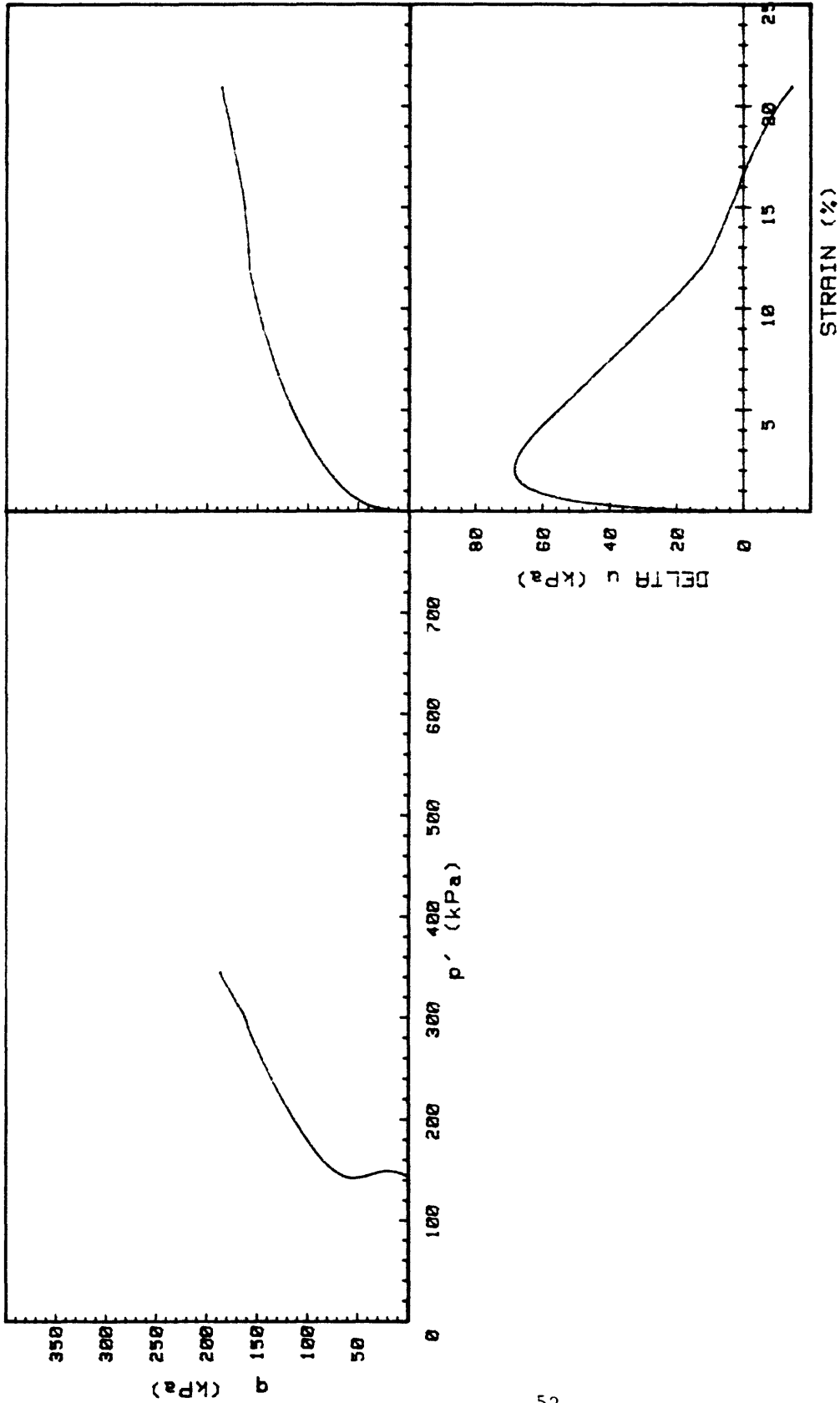
KSI-83-CS	INCREMENT (cm)	S-43E
CORE NO. B-3	TEST NO.	TE271
SIG1c' (kPa)	476.5	
SIG3c' (kPa)	476.5	
INDUCED OCR	1.0	



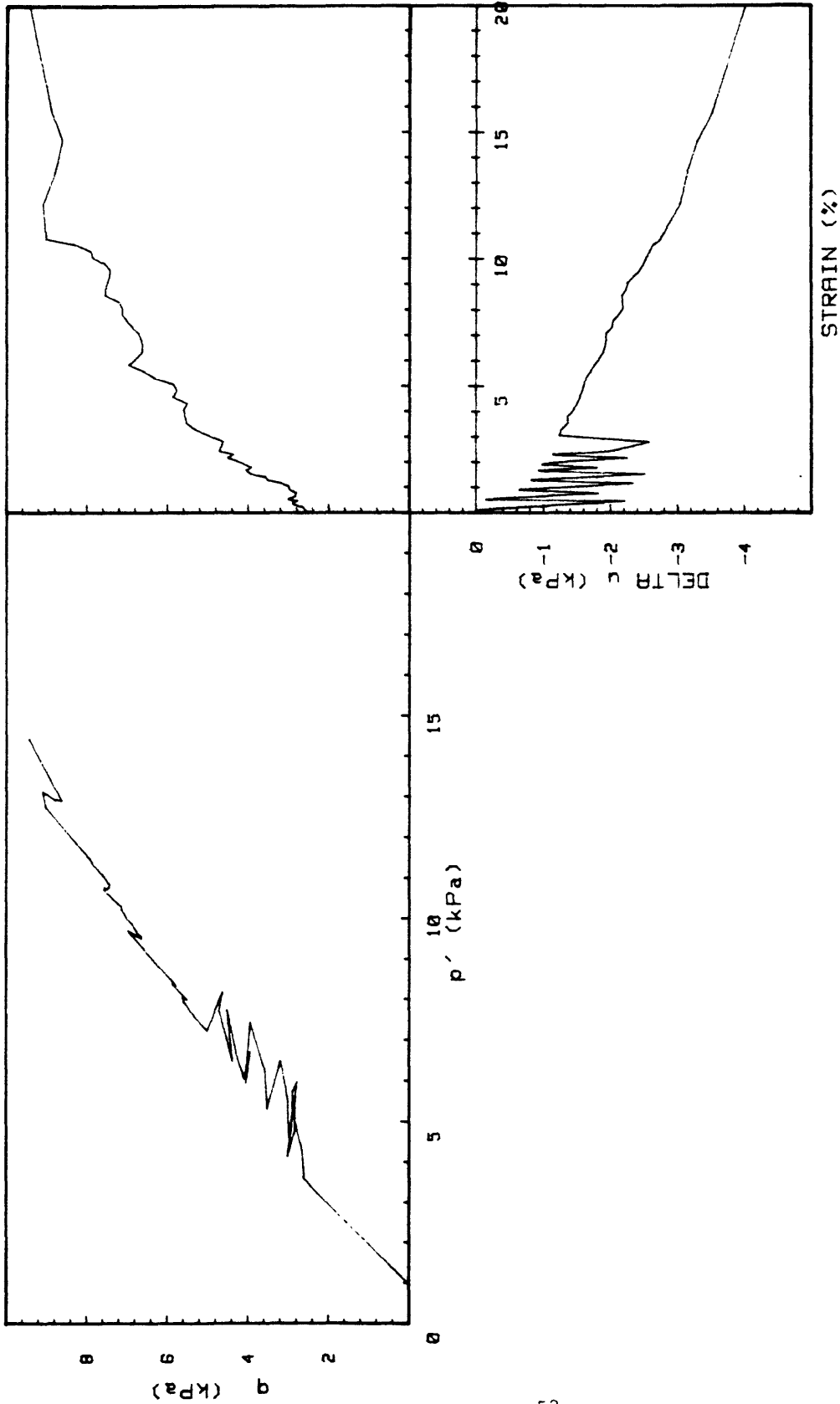
KSI-83-CS	INCREMENT (cm)	SEC- 1
CORE NO. B7	TEST NO.	TE261
SIG1c' (kPa)	4.2	
SIG3c' (kPa)	4.2	
INDUCED OCR	1	



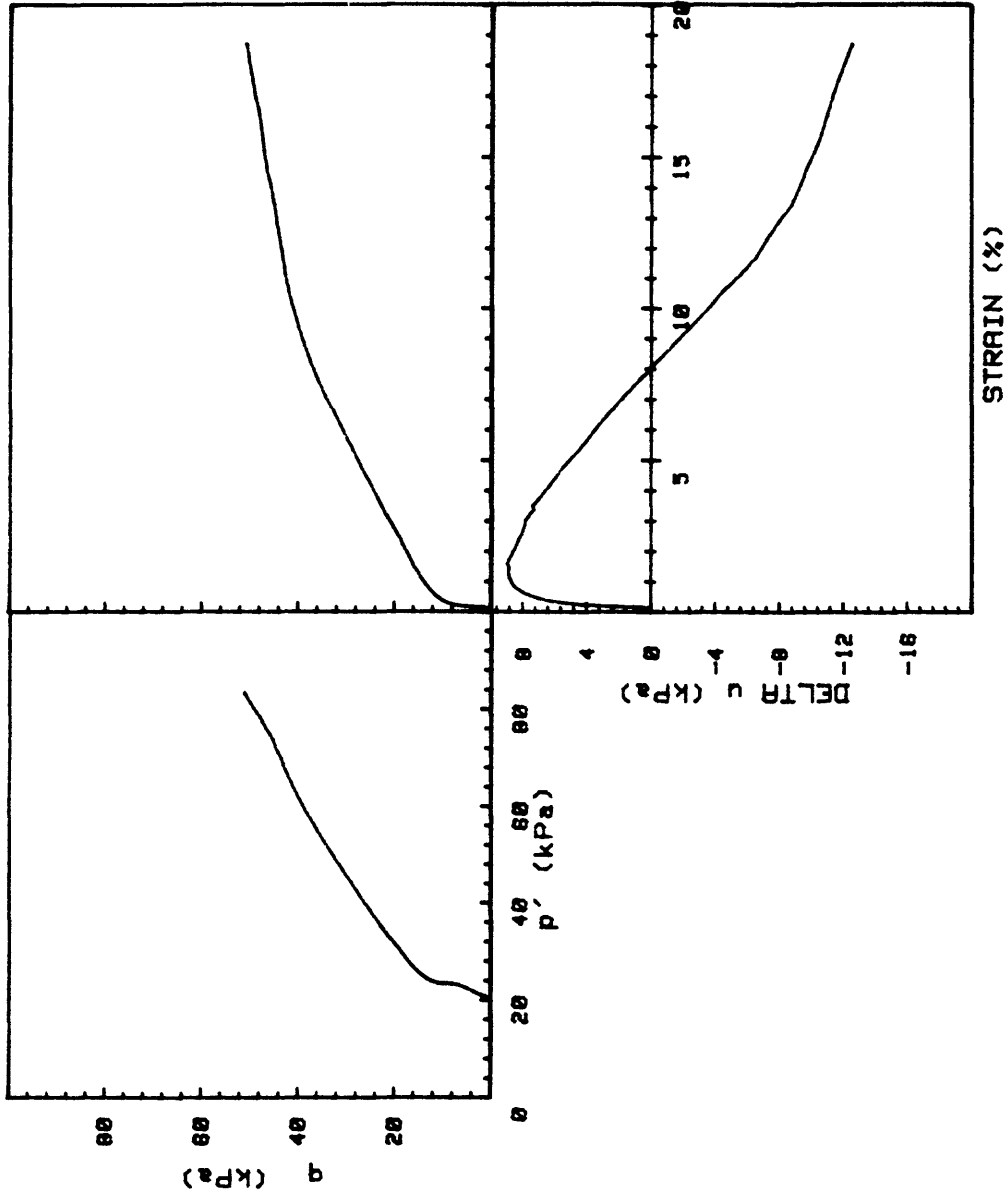
KSI-83-CS	INCREMENT (cm)	SEC-21
CORE NO. B-7	TEST NO.	TE262
SIG1c' (kPa)	123.5	
SIG3c' (kPa)	123.5	
INDUCED OCR	1	



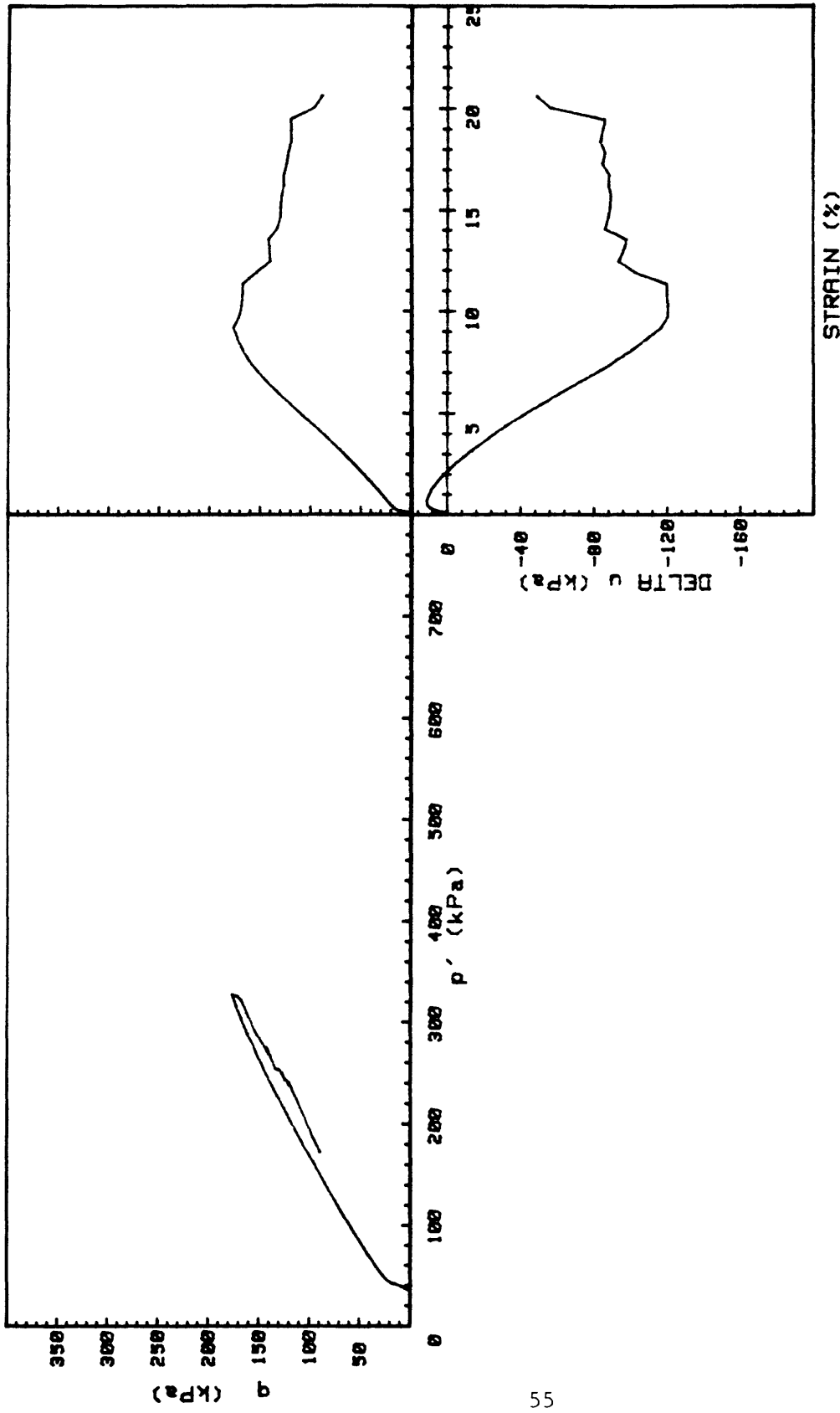
KSI-83-CS	INCREMENT (cm)	SEC-24
CORE NO. B -7	TEST NO.	TE263
SIG1c' (kPa)	144.3	
SIG3c' (kPa)	144.3	
INDUCED OCR	1	



KSI-83-CS	INCREMENT (cm)	S-1
CORE NO. B-8	TEST NO.	TE269
SIG1c' (kPa)	1.0	
SIG3c' (kPa)	1.0	
INDUCED OCR	N/A	



KSI-83-CS	INCREMENT (cm)	S-4
CORE NO. 8	TEST NO.	TE225
SIG1c' (kPa)	19.9	
SIG3c' (kPa)	19.9	
INDUCED OCR	1.0	



KSI-83-CS	INCREMENT (cm)	S-6
CORE NO. 8	TEST NO.	TE226
SIG1c' (kPa)	34.7	
SIG3c' (kPa)	34.7	
INDUCED OCR	1.0	